REFERENCES

[1] W. P. Ayres, P. H. Vartanian, and J. L. Melchor, "Frequency doubling in ferrites," *J. Appl. Phys.*, vol. 27, pp. 188–189, Feb. 1956.
[2] J. E. Pippin, "Frequency doubling and mixing in ferrites," Gordon McKay Lab., Harvard Univ., Cambridge, MA, Sci. Rep. 2, AFCRL-TN-56-369, May 5, 1956.
[3] J. L. Melchor, W. P. Ayres, and P. H. Vartanian, "Microwave frequency doubling from 9 to 18 KMC in ferrites," *Proc. IRE*, vol. 45, pp. 643–646, May 1957.
[4] R. L. Jepsen, "Harmonic generation and frequency mixing in ferromagnetic insulators," *J. Appl. Phys.*, vol. 32, pp. 2627–2630, Dec. 1961.
[5] R. T. Denton, "A ferromagnetic amplifier using longitudinal pumping," *Proc. IRE* (Corresp.), vol. 48, pp. 937–938, May 1960.
[6] H. Suhl, "Theory of the ferromagnetic microwave amplifier," *J. Appl. Phys.*, vol. 28, pp. 1225–1236, Nov. 1957.
[7] M. T. Weiss, "A solid-state microwave amplifier and oscillator using ferrites," *Phys. Rev.*, vol. 107, p. 317, July 1957.
[8] H. Suhl, "The nonlinear behavior of ferrites at high microwave signal levels," *Proc. IRE*, vol. 44, pp. 1270–1284, Oct. 1956.
[9] L. Landau and E. Lifschitz, "On the theory of the dispersion of magnetic permeability in ferromagnetic bodies," *Phys. Z. Sowjetunion*, vol. 8, p. 153, 1935.
[10] D. Polder, "On the theory of ferromagnetic resonance," *Phil. Mag.*, vol. 40, pp. 99–115, Jan. 1949.
[11] J. Helszajn, *Principles of Microwave Ferrite Engineering.* New York: Wiley-Interscience, 1969.
[12] H. Bosma, "On stripline Y-circulation at UHF," *IEEE Trans. Microwave Theory Tech.* (*1963 Symposium Issue*), vol. MTT-12, pp. 61–72, Jan. 1964.
[13] C. E. Fay and R. L. Comstock, "Operation of the ferrite junction circulator," *IEEE Trans. Microwave Theory Tech.* (*1964 Symposium Issue*), vol. MTT-13, pp. 15–27, Jan. 1965.
[14] Y. S. Wu and F. J. Rosenbaum, "Wide-band operation of microstrip circulators," *IEEE Trans. Microwave Theory Tech.*, vol. MTT-22, pp. 849–856, Oct. 1974.
[15] M. Abramoritz and I. A. Segun, *Handbook of Mathematical Functions.* New York: Dover, 1965.
[16] R. E. Collins, *Foundations of Microwave Engineering.* New York: McGraw-Hill, 1966.
[17] Y. Konishi, "Lumped element Y circulator" *IEEE Trans. Microwave Theory Tech.* (*1965 Symposium Issue*), vol. MTT-13, pp. 852–864, Nov. 1965.
[18] Y. Konishi, "A high-power UHF circulator," *IEEE Trans. Microwave Theory Tech.* (*1967 Symposium Issue*), vol. MTT-15, pp. 700–708, Dec. 1967.

A Theoretical Study of Light Beams Guided Along Tapered Lenslike Media, and Their Applications

SHINNOSUKE SAWA, MEMBER, IEEE

***Abstract*—Propagation behavior of light beams along the tapered lenslike media, in which both the focusing parameter and the on-axis permittivity have gradients in the axial direction, is investigated in detail, theoretically and numerically, with the help of the approximate wave theory. As a result, it is clarified that the tapered lenslike media can be classified into two kinds, according to the differences of the focusing property. Matched incidence conditions to eliminate the fluctuations of the light beam are also clarified. As an application of the theory, a spot-size transducer and a mode transducer for use in a circular bend of the light focusing waveguide are proposed, and the design conditions are derived. A ray-oscillation suppressor (ROS) is also proposed, and its applicability to some new optical circuit components is discussed.**

Manuscript received April 7, 1975; revised August 7, 1975. This work was supported by the Science Research Fund of the Ministry of Education. Numerical calculations were done on FACOM 230-60 at the Data Processing Center, Kyoto University, and NEAC 2200-700·500 at the Computer Center, Osaka University.

The author is with the Department of Electronics, Faculty of Engineering, Ehime University, Matsuyama City, 790 Japan.

I. INTRODUCTION

OPTICAL waveguides such as parabolic-index fibers termed SELFOC [1] are technologically important because of the applicability to optical communication, optical instruments, and optical date processing. As is well known, waveguides of this type consist of a lenslike medium whose permittivity decreases quadratically with distance in the transverse direction from the guide axis.

The lenslike medium with a permittivity profile varying not only in the transverse direction but also in the direction of the guide axis may be termed a "tapered lenslike medium." The tapered lenslike medium is expected to have various interesting applications to optical circuit components, since it has a light-focusing property varying slowly and continuously along the axial direction.

Several papers have already been reported on the tapered lenslike media [2]–[6]. For example, Tien *et al.*

[2] have already analyzed the propagation behavior of a Gaussian beam along lenslike media of various forms by the viewpoint of ray theory, and have derived the basic equations for the spot size and the curvature of the phase front of the light beam as well as the trajectory of the beam center in the tapered lenslike media. In the previous papers [2]–[6], however, some interesting and important focusing properties of the tapered lenslike media have not yet been clarified satisfactorily.

In the present paper we deal with the tapered lenslike media from the wave theory point of view, unlike the viewpoint of ray theory as in the previous papers [2]–[6]. We consider a tapered lenslike medium in which both the on-axis permittivity and the focusing parameter determining the rate of change of the permittivity in the transverse direction have gradients in the axial direction.

General expressions for the response of the electromagnetic fields in the tapered medium with a taper of arbitrary shape are derived, with the help of an approximate wave theory previously described [7]–[9]. The results are applied to the cases of various tapers. For convenience, the tapered lenslike media are classified into two kinds. One is a "tapered lenslike medium of the first kind," and the other is a "tapered lenslike medium of the second kind." As a typical example of the first kind of tapered lenslike medium, we consider the simplified case in which the focusing parameter has a gradient in the axial direction, while the on-axis permittivity is constant. For this case, the linearly, exponentially, and raised-cosine-wise tapered media are studied. As for the second kind of tapered lenslike medium, we take the simplest case in which the on-axis permittivity has a gradient varying exponentially in the axial direction, whereas the focusing parameter is constant.

Propagation behavior of light beams for these cases is investigated in detail theoretically and numerically. As a result, it is clarified that the two kinds of tapered media possess different focusing properties. For example, the second kind of tapered lenslike medium possesses the following two interesting characteristics which are not found in the simplified case of the first kind of tapered medium where the on-axis permittivity is assumed to be constant. 1) The light beam exhibits three types of responses—oscillatory, nonoscillatory, and critically damped responses—according to the differences of the axial gradient given to the focusing parameter and the on-axis permittivity. 2) The undulations of the beam trajectory and its slope, as well as the fluctuation of the spot size of the light beam, decrease (or increase) in amplitude with increasing propagation distance. Further, matched incidence conditions to eliminate the fluctuation of the spot size as well as the undulation of the beam trajectory are derived. As an appliction of the theory, a spot-size transducer and a mode transducer for use in a circular bend of the light focusing waveguide are proposed, which are composed of the first kind of tapered medium with a raised-cosine taper, and the design conditions for both transducers are clarified. As a further application, a ray-oscillation suppressor (ROS) using the second kind of tapered medium is proposed, and its applicability to some new optical circuit components is considered.

For simplicity, the analysis in the present paper is limited to a two-dimensional model, and it is based on the Wentzel–Kramers–Brillouin–Jeffreys (WKBJ) method [10] and a paraxial beam approximation.

II. BASIC EQUATION AND ITS SOLUTIONS

A. Straight Section

We consider a straight section of the tapered lenslike medium as shown in Fig. 1(a) and assume the permittivity profile to be

$$\epsilon(x,z) = \epsilon(0)G^2(z)\{1 - g^2(z)x^2\} \tag{1}$$

where $\epsilon(0)G^2(z)$ represents the on-axis permittivity of the medium along $x = 0$ and $g(z)$ is the focusing parameter. Both $G(z)$ and $g(z)$ are assumed to be the functions of z alone, varying very slowly in the axial z direction. In the following, it is assumed that the permittivity $\epsilon(x,z)$ varies so slowly in both the x and z directions that its variations over a distance of a free-space wavelength λ_0 of a light wave can be neglected.

Electromagnetic fields of a light wave propagating along such media are derived approximately from the scalar wave equation [7]

$$\frac{\partial^2 V}{\partial x^2} + \frac{\partial^2 V}{\partial z^2} + k^2(0)G^2(z)\{1 - g^2(z)x^2\}V = 0 \tag{2}$$

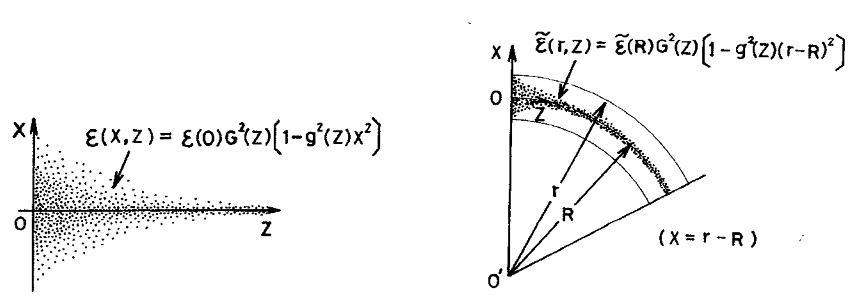

(a) (b)

Fig. 1. Straight and circularly bent sections of the tapered lenslike medium. (a) Straight section in which permittivity $\epsilon(x,z)$ is given by (1). (b) Circularly bent section in which permittivity $\tilde{\epsilon}(r,z)$ is given by (16).

where

$$k(0) = \omega[\mu\epsilon(0)]^{1/2} \tag{3}$$

and μ is the permeability of the medium, and sinusoidal time dependence with angular frequency ω is assumed.

Since we are interested in the waves propagating primarily in the axial z direction, in other words, the almost plane waves, let us write

$$V = U(x,z) \exp\left[-jk(0) \int G(z)\, dz\right]. \tag{4}$$

We assume that the field distribution function $U(x,z)$ varies so slowly with z that its second derivative with respect to z is negligibly small. Substituting (4) in (2) and neglecting the second derivative $\partial^2U(x,z)/\partial z^2$, we obtain the paraxial wave equation

$$\frac{\partial^2 U}{\partial x^2} - j2K(z)\frac{\partial U}{\partial z} - \{K'(z) + K^2(z)g^2(z)x^2\}U = 0 \tag{5}$$

with

$$K(z) = k(0)G(z) \tag{6}$$

where the prime indicates the differentiation with respect to z.

In order to clarify the behavior of the light beam propagating along the medium whose permittivity varies parabolically in the transverse plane as given by (1), it is essential to analyze the propagation behavior of Hermite–Gaussian beams. Thus let us consider an Hermite–Gaussian beam having input wavefront coefficient[1] $1/S^2(0)$ as well as the input slope $\delta'(0)$ and the input displacement $\delta(0)$ of the beam center from the center axis of the medium (the optic axis) $x = 0$, at the entrance of the tapered medium $z = 0$:

$$U(x,0) = \exp\left[-\frac{\{x-\delta(0)\}^2}{2S^2(0)} - jK(0)\delta'(0)x\right] \cdot \mathrm{He}_n\left[\frac{x-\delta(0)}{S(0)}\right]. \tag{7}$$

[1] The wavefront coefficient used in this paper is defined as

$$1/S^2(z) = 1/w^2(z) + j\,K(z)/R(z)$$

where $w(z)$ and $R(z)$ represent, respectively, the spot size and the radius of phase front curvature of a Gaussian beam. This coefficient can also be related to the well-known complex beam parameter $1/q(z)$ [11] as $1/S^2(z) = jK(z)/q(z)$.

Following the convenient method of analysis devised so far [7]–[9] (see the Appendix), we can determine the field distribution function $U(x,z)$ from (5). As a result, the primary parameters which govern the propagation behavior of the light beam, i.e., the wavefront coefficient $1/S^2(z)$, the trajectory of the beam center $\delta(z)$, and its slope $\delta'(z)$ are derived as follows:

$$\frac{1}{S^2(z)} = \frac{h(z)}{S^2(0)} \cdot \frac{\lambda_2(0)p_1(z) - \lambda_1(0)p_2(z) - jK(0)S^2(0)\{p_1(0)p_2(z) - p_2(0)p_1(z)\}}{p_1(0)\lambda_2(z) - p_2(0)\lambda_1(z) - jK^{-1}(0)S^{-2}(0)\{\lambda_1(0)\lambda_2(z) - \lambda_2(0)\lambda_1(z)\}} \tag{8}$$

$$\delta(z) = \frac{\{p_2(0)\lambda_1(z) - p_1(0)\lambda_2(z)\}\delta(0) - \{\lambda_2(0)\lambda_1(z) - \lambda_1(0)\lambda_2(z)\}\delta'(0)}{[h(z)]^{1/2}\{\lambda_1(0)p_2(0) - \lambda_2(0)p_1(0)\}} \tag{9}$$

$$\delta'(z) = -\frac{\{p_2(0)p_1(z) - p_1(0)p_2(z)\}\delta(0) + \{\lambda_2(0)p_1(z) - \lambda_1(0)p_2(z)\}\delta'(0)}{[h(z)]^{1/2}\{\lambda_1(0)p_2(0) - \lambda_2(0)p_1(0)\}} \tag{10}$$

with

$$p_i(z) = \frac{K'(z)}{2K(z)}\lambda_i(z) - \lambda_i'(z), \qquad i = 1,2 \tag{11}$$

$$h(z) = \frac{K(z)}{K(0)} = \frac{G(z)}{G(0)}. \tag{12}$$

In the foregoing equations (8)–(11), the functions $\lambda_1(z)$ and $\lambda_2(z)$ represent the two independent solutions of

$$\frac{d^2\lambda(z)}{dz^2} + [g^2(z) - \sigma'(z) - \sigma^2(z)]\lambda(z) = 0 \tag{13}$$

where

$$\sigma(z) = \frac{G'(z)}{2G(z)} \quad \sigma'(z) = \frac{d\sigma(z)}{dz}. \tag{14}$$

The spot size $w(z)$ of the Gaussian beam can be obtained from the real part of $1/S^2(z)$ given by (8), as

$$w(z) = 1/[\mathrm{Re}\{1/S^2(z)\}]^{1/2}. \tag{15}$$

B. Circularly Bent Section

Next we consider the case where the center axis of the tapered lenslike medium is curved in a circular bend with the radius of curvature R, as shown in Fig. 1(b). Let the permittivity profile for this case be

$$\tilde{\epsilon}(r,z) = \tilde{\epsilon}(R)G^2(z)\{1 - g^2(z)(r-R)^2\} \tag{16}$$

and let the radius of curvature R be large enough to satisfy the inequality

$$|r - R| \ll R. \tag{17}$$

Under the same assumptions as in the case of the straight section, we can derive the expression for the distribution function of the electromagnetic fields. The result yields the primary parameters, i.e., the wavefront coefficient $1/\tilde{S}^2(z)$, the trajectory of the beam center $\tilde{\delta}(z)$, and its slope $\tilde{\delta}'(z)$ as

$$\frac{1}{\tilde{S}^2(z)} = \frac{h(z)}{S^2(0)} \cdot \frac{\tilde{\lambda}_2(0)\tilde{p}_1(z) - \tilde{\lambda}_1(0)\tilde{p}_2(z) - j\tilde{K}(0)S^2(0)\{\tilde{p}_1(0)\tilde{p}_2(z) - \tilde{p}_2(0)\tilde{p}_1(z)\}}{\tilde{p}_1(0)\tilde{\lambda}_2(z) - \tilde{p}_2(0)\tilde{\lambda}_1(z) - j\tilde{K}^{-1}(0)S^{-2}(0)\{\tilde{\lambda}_1(0)\tilde{\lambda}_2(z) - \tilde{\lambda}_2(0)\tilde{\lambda}_1(z)\}} \tag{18}$$

$$\tilde{\delta}(z) = \frac{\{\tilde{p}_2(0)\tilde{\lambda}_1(z) - \tilde{p}_1(0)\tilde{\lambda}_2(z)\}\delta(0) - \{\tilde{\lambda}_2(0)\tilde{\lambda}_1(z) - \tilde{\lambda}_1(0)\tilde{\lambda}_2(z)\}\{\delta'(0) - \delta_c'(0)\}}{[h(z)]^{1/2}\{\tilde{\lambda}_1(0)\tilde{p}_2(0) - \tilde{\lambda}_2(0)\tilde{p}_1(0)\}} + \delta_c(z) \tag{19}$$

$$\tilde{\delta}'(z) = -\frac{\{\tilde{p}_2(0)\tilde{p}_1(z) - \tilde{p}_1(0)\tilde{p}_2(z)\}\delta(0) + \{\tilde{\lambda}_2(0)\tilde{p}_1(z) - \tilde{\lambda}_1(0)\tilde{p}_2(z)\}\{\delta'(0) - \delta_c'(0)\}}{[h(z)]^{1/2}\{\tilde{\lambda}_1(0)\tilde{p}_2(0) - \tilde{\lambda}_2(0)\tilde{p}_1(0)\}} + \delta_c'(z) \tag{20}$$

with

$$\tilde{p}_i(z) = \frac{\tilde{K}'(z)}{2\tilde{K}(z)}\tilde{\lambda}_i(z) - \tilde{\lambda}_i'(z), \qquad i = 1,2 \tag{21}$$

$$\delta_c(z) = \frac{1}{R[\tilde{K}(z)]^{1/2}} \int_0^z \frac{\tilde{\lambda}_1(\eta)\tilde{\lambda}_2(z) - \tilde{\lambda}_1(z)\tilde{\lambda}_2(\eta)}{\tilde{\lambda}_1(\eta)\tilde{\lambda}_2'(\eta) - \tilde{\lambda}_1'(\eta)\tilde{\lambda}_2(\eta)}\, d\eta \tag{22}$$

$$\delta_c'(z) = \frac{d}{dz}\delta_c(z) \tag{23}$$

where

$$\tilde{K}(z) = \tilde{k}(0)G(z) \quad \tilde{k}(0) = \omega[\mu\tilde{\epsilon}(R)]^{1/2}. \tag{24}$$

In the preceding equations (18)–(22), $\tilde{\lambda}_1(z)$ and $\tilde{\lambda}_2(z)$ are the two independent solutions of

$$\frac{d^2\tilde{\lambda}(z)}{dz^2} + [\tilde{g}^2(z) - \sigma'(z) - \sigma^2(z)]\tilde{\lambda}(z) = 0 \tag{25}$$

where

$$\tilde{g}(z) = g(z)\left(1 - \frac{2}{g^2(z)R^2}\right)^{1/2}. \tag{26}$$

The spot size $\tilde{w}(z)$ of the Gaussian beam can be derived from (18) as

$$\tilde{w}(z) = 1/[\mathrm{Re}\,\{1/\tilde{S}^2(z)\}]^{1/2}. \tag{27}$$

dent. The other is the second kind, in which $G(z)$ and $g(z)$ have a fixed relation.

A. Tapered Lenslike Medium of the First Kind

For this kind of tapered lenslike medium, the coefficient of the second term of the left-hand side of (13), $g^2(z) - \sigma'(z) - \sigma^2(z)$, is in general a function of z. Therefore, (13) can be represented as

$$\frac{d^2\lambda(z)}{dz^2} + T^2(z)\lambda(z) = 0 \tag{28}$$

with

$$T(z) = [g^2(z) - \sigma'(z) - \sigma^2(z)]^{1/2}. \tag{29}$$

As mentioned in the preceding, we have assumed that $G(z)$ and $g(z)$ are slowly varying functions of z, so that the function $T(z)$ defined by (29) can also be considered to be a slowly varying function of z. Thus let us further assume

$$\frac{1}{T^2(z)}\left|\frac{d^2T(z)}{dz^2}\right| \ll 1. \tag{30}$$

Then we can solve (28) by the use of WKBJ approximation [10]. Adopting the solutions thus obtained as the two independent solutions $\lambda_1(z)$ and $\lambda_2(z)$, we can express the field distribution function $U(x,z)$ for the straight section as

$$U(x,z) = \exp\left[-\frac{\{x-\delta(z)\}^2}{2S^2(z)} - jK(z)\delta'(z)x + j\{K(z)\delta(z)\delta'(z) - K(0)\delta(0)\delta'(0)\}\right]$$
$$\cdot \frac{\left(\cos g_0\theta + u(0)\sin g_0\theta + j\dfrac{w_c^2}{S^2(0)}\sin g_0\theta\right)^{n/2}}{\left(\cos g_0\theta + u(0)\sin g_0\theta - j\dfrac{w_c^2}{S^2(0)}\sin g_0\theta\right)^{(n+1)/2}} \cdot \rho^{1/4}(z) \cdot h^{-1/2}(z)$$
$$\cdot \mathrm{He}_n\left[\frac{\{x-\delta(z)\}[\rho(z)]^{1/2}/S(0)}{\left(\{\cos g_0\theta + u(0)\sin g_0\theta\}^2 + \dfrac{w_c^4}{S^4(0)}\sin^2 g_0\theta\right)^{1/2}}\right] \tag{31}$$

where $\mathrm{He}_n(x)$ refers to the Hermite polynomial of the nth order defined by (A2) in the Appendix. The parameters used in (31) are given in Table I. In a similar fashion, we can get the field distribution function for the circularly bent section by replacing $1/S^2(z)$, $\delta(z)$, $\delta'(z)$, $\rho(z)$, $u(z)$, θ, $K(z)$, g_0, and w_c in (31) with $1/\tilde{S}^2(z)$, $\tilde{\delta}(z)$, $\tilde{\delta}'(z)$, $\tilde{\rho}(z)$, $\tilde{u}(z)$, $\tilde{\theta}$, $\tilde{K}(z)$, $\tilde{g}_0$, and $\tilde{w}_c$, which are also listed in Table I except for $\tilde{K}(z)$ given by (24).

III. PROPAGATION BEHAVIOR OF LIGHT BEAMS ALONG TAPERED LENSLIKE MEDIA

For convenience, let the tapered lenslike media be classified into the following two kinds. One is the first kind of tapered lenslike medium, in which the parameters $G(z)$ and $g(z)$ governing the shape of taper are indepen-

TABLE I

PRIMARY PARAMETERS GOVERNING THE PROPAGATION BEHAVIOR OF LIGHT BEAMS ALONG THE TAPERED LENSLIKE MEDIUM OF THE FIRST KIND

	Straight Section	Circularly Bent Section
Wave Front Coefficient	$\frac{1}{S^2(z)} = \frac{\rho(z)}{S^2(0)} \cdot \frac{\cos g_0\theta - u(z)\sin g_0\theta - j\frac{S^2(0)}{W_c^2}\left[\{1+u(0)u(z)\}\sin g_0\theta + \{u(z)-u(0)\}\cos g_0\theta\right]}{\cos g_0\theta + u(0)\sin g_0\theta - j\frac{W_c^2}{S^2(0)}\sin g_0\theta}$	$\frac{1}{\tilde{S}^2(z)} = \frac{\tilde{\rho}(z)}{S^2(0)} \cdot \frac{\cos\tilde{g}_0\tilde{\theta} - \tilde{u}(z)\sin\tilde{g}_0\tilde{\theta} - j\frac{S^2(0)}{\tilde{W}_c^2}\left[\{1+\tilde{u}(0)\tilde{u}(z)\}\sin\tilde{g}_0\tilde{\theta} + \{\tilde{u}(z)-\tilde{u}(0)\}\cos\tilde{g}_0\tilde{\theta}\right]}{\cos\tilde{g}_0\tilde{\theta} + \tilde{u}(0)\sin\tilde{g}_0\tilde{\theta} - j\frac{\tilde{W}_c^2}{S^2(0)}\sin\tilde{g}_0\tilde{\theta}}$
Trajectory of the Beam Center	$\delta(z) = \rho^{-1/2}(z)\left[\delta(0)\{\cos g_0\theta + u(0)\sin g_0\theta\} + \frac{\delta'(0)}{g_0}\sin g_0\theta\right]$	$\tilde{\delta}(z) = \tilde{\rho}^{-1/2}(z)\left[\delta(0)\{\cos\tilde{g}_0\tilde{\theta} + \tilde{u}(0)\sin\tilde{g}_0\tilde{\theta}\} + \left\{\frac{\delta'(0)-\delta_c'(0)}{\tilde{g}_0}\right\}\sin\tilde{g}_0\tilde{\theta}\right] + \delta_c(z)$
Slope of the Beam Trajectory	$\delta'(z) = -g_0\sqrt{\frac{v(z)}{h(z)}}\left[\delta(0)\left[\{1+u(0)u(z)\}\sin g_0\theta + \{u(z)-u(0)\}\cos g_0\theta\right] + \frac{\delta'(0)}{g_0}\{u(z)\sin g_0\theta - \cos g_0\theta\}\right]$	$\tilde{\delta}'(z) = -\tilde{g}_0\sqrt{\frac{\tilde{v}(z)}{h(z)}}\left[\delta(0)\left[\{1+\tilde{u}(0)\tilde{u}(z)\}\sin\tilde{g}_0\tilde{\theta} + \{\tilde{u}(z)-\tilde{u}(0)\}\cos\tilde{g}_0\tilde{\theta}\right] + \left\{\frac{\delta'(0)-\delta_c'(0)}{\tilde{g}_0}\right\}\{\tilde{u}(z)\sin\tilde{g}_0\tilde{\theta} - \cos\tilde{g}_0\tilde{\theta}\}\right] + \delta_c'(z)$
Spot Size	$W(z) = \left[\frac{1}{2}\left[1+u^2(0)+\left\lvert\frac{W_c}{S(0)}\right\rvert^4 + \left\{1-u^2(0)-\left\lvert\frac{W_c}{S(0)}\right\rvert^4\right\}\cos 2g_0\theta + 2u(0)\sin 2g_0\theta\right] + \{u(0)(1-\cos 2g_0\theta) + \sin 2g_0\theta\}\cdot \mathrm{Im}\left\{\frac{W_c^2}{S^2(0)}\right\}\right]^{1/2} \Big/ \left[\frac{\rho(z)}{W_c^2}\cdot \mathrm{Re}\left\{\frac{W_c^2}{S^2(0)}\right\}\right]^{1/2}$	$\tilde{W}(z) = \left[\frac{1}{2}\left[1+\tilde{u}^2(0)+\left\lvert\frac{\tilde{W}_c}{S(0)}\right\rvert^4 + \left\{1-\tilde{u}^2(0)-\left\lvert\frac{\tilde{W}_c}{S(0)}\right\rvert^4\right\}\cos 2\tilde{g}_0\tilde{\theta} + 2\tilde{u}(0)\sin 2\tilde{g}_0\tilde{\theta}\right] + \{\tilde{u}(0)(1-\cos 2\tilde{g}_0\tilde{\theta}) + \sin 2\tilde{g}_0\tilde{\theta}\}\cdot \mathrm{Im}\left\{\frac{\tilde{W}_c^2}{S^2(0)}\right\}\right]^{1/2} \Big/ \left[\frac{\tilde{\rho}(z)}{\tilde{W}_c^2}\cdot \mathrm{Re}\left\{\frac{\tilde{W}_c^2}{S^2(0)}\right\}\right]^{1/2}$
Parameters Used in the Expressions	$v(z) = T(z)/T(0)$, $h(z) = G(z)/G(0)$, $g_0 = T(0)$, $u(z) = \frac{1}{2g_0 v(z)}\left\{\frac{v'(z)}{v(z)} + \frac{h'(z)}{h(z)}\right\}$, $\rho(z) = v(z)h(z)$, $\theta = \int_0^z v(\eta)d\eta$, $W_c = 1/\sqrt{g_0 k(0)}$	$\tilde{v}(z) = \tilde{T}(z)/\tilde{T}(0)$, $h(z) = G(z)/G(0)$, $\tilde{g}_0 = \tilde{T}(0)$, $\tilde{u}(z) = \frac{1}{2\tilde{g}_0\tilde{v}(z)}\left\{\frac{\tilde{v}'(z)}{\tilde{v}(z)} + \frac{h'(z)}{h(z)}\right\}$, $\tilde{\rho}(z) = \tilde{v}(z)h(z)$, $\tilde{\theta} \equiv \tilde{\theta}(z) = \int_0^z \tilde{v}(\eta)d\eta$, $\tilde{W}_c = 1/\sqrt{\tilde{g}_0\tilde{k}(0)}$, $\delta_c(z) = \frac{\tilde{\rho}^{-1/2}(z)}{\tilde{g}_0 R}\int_0^z \frac{\sin\tilde{g}_0\{\tilde{\theta}(z)-\tilde{\theta}(\eta)\}}{\tilde{v}(\eta)}d\eta$

Note: The parameters $G(z)$ and $g(z)$ are independent.

As a typical example, let us consider the simplified case that $G(z)$ = constant and $g(z)$ is a function of z. In this case, $\sigma(z)$ of (14) becomes zero and hence (29) is simplified to $T(z) = g(z)$. Such a tapered medium may be termed a "prototype of tapered lenslike medium of the first kind." Let us restrict our attention to this prototype and investigate the propagation behavior of light beams in detail, according to the following examples.

1) Linear Taper: We consider the simplest model of this kind of medium, a linear taper, which is defined by the functions

$$G(z) = 1 \quad g(z) = g_0(az + 1) \tag{32}$$

where a is a constant, and $g_0 > 0$.

The field distribution function $U(x,z)$ for the input beam of (7) is obtained by substituting into (31) $\rho(z) \sim w_c$ in (I) of Table II for the straight section and $\tilde{\rho}(z) \sim \tilde{w}_c$ in (I) of the same table for the circularly bent section, together with the expressions given in Table I. As a result, the trajectory of the beam center $\delta(z)$, its slope $\delta'(z)$, and the spot size of the Gaussian beam $w(z)$ are expressed for the straight section as

$$\delta(z) = \frac{1}{(az+1)^{1/2}}\left[\left\{\cos g_0\theta + \frac{a}{2g_0}\sin g_0\theta\right\}\delta(0) + \frac{\delta'(0)}{g_0}\sin g_0\theta\right] \tag{33}$$

$$\delta'(z) = (az+1)^{1/2}\left[\left[\frac{1}{2}a\left\{1 - \frac{1}{(az+1)^2}\right\}\cos g_0\theta - g_0\left\{1 + \frac{a^2}{4g_0^2(az+1)^2}\right\}\cdot\sin g_0\theta\right]\delta(0) + \left\{\cos g_0\theta - \frac{a\sin g_0\theta}{2g_0(az+1)^2}\right\}\delta'(0)\right] \tag{34}$$

$$w(z) = \frac{w(0)}{(az+1)^{1/2}}\left[\frac{1}{2}\left\{1 + \frac{w_c^4}{\lvert S(0)\rvert^4} + \left(1 - \frac{w_c^4}{\lvert S(0)\rvert^4}\right)\cos 2g_0\theta + \frac{a}{g_0}\sin 2g_0\theta + \frac{a^2(1-\cos 2g_0\theta)}{4g_0^2}\right\} + \left\{\frac{a(1-\cos 2g_0\theta)}{2g_0} + \sin 2g_0\theta\right\}\cdot \mathrm{Im}\left\{\frac{w_c^2}{S^2(0)}\right\}\right]^{1/2} \tag{35}$$

and $\tilde{\delta}(z)$ and $\tilde{w}(z)$ for the circularly bent section as

TABLE II
PARAMETERS FOR DETERMINING THE RESPONSE OF THE ELECTROMAGNETIC FIELDS OF THE LIGHT BEAM GUIDED ALONG THE TAPERED LENSLIKE MEDIUM OF THE FIRST KIND WITH LINEAR, EXPONENTIAL, AND RAISED-COSINE TAPERS

Shape of taper	Straight Section		Circularly Bent Section	
(I) Linear Taper	$\varrho(z)$	$az+1$	$\tilde{\varrho}(z)$	$\sqrt{(az+1)^2-\gamma^2}/\sqrt{1-\gamma^2}$
	$u(z)$	$\dfrac{a}{2g_0(az+1)^2}$	$\tilde{u}(z)$	$a(az+1)/[2g_0\{\sqrt{(az+1)^2-\gamma^2}\}^3]$
	θ	$\dfrac{az^2}{2}+z$	$\tilde{\theta}$	$\dfrac{1}{2a}\Big[(az+1)\sqrt{(az+1)^2-\gamma^2}/\sqrt{1-\gamma^2}-1-\dfrac{\gamma^2}{\sqrt{1-\gamma^2}}\ln\Big\lvert\dfrac{az+1+\sqrt{(az+1)^2-\gamma^2}}{1+\sqrt{1-\gamma^2}}\Big\rvert\Big]$
	g_0	$g(0)$	$\tilde{g}_0$	$g_0\sqrt{1-\gamma^2}$
	w_c	$1/\sqrt{g(0)k(0)}$	$\tilde{w}_c$	$w_c/\sqrt[4]{1-\gamma^2}$
(II) Exponential Taper	$\varrho(z)$	e^{az}	$\tilde{\varrho}(z)$	$\sqrt{e^{2az}-\gamma^2}/\sqrt{1-\gamma^2}$
	$u(z)$	$\dfrac{a e^{-az}}{2g_0}$	$\tilde{u}(z)$	$a e^{2az}/[2g_0\{e^{2az}-\gamma^2\}^{3/2}]$
	θ	$\dfrac{e^{az}-1}{a}$	$\tilde{\theta}$	$\dfrac{1}{a}\Big[\sqrt{e^{2az}-\gamma^2}/\sqrt{1-\gamma^2}-1+\dfrac{\gamma}{\sqrt{1-\gamma^2}}\Big\{\mathrm{Cosec}^{-1}\dfrac{e^{az}}{\gamma}-\mathrm{Cosec}^{-1}\dfrac{1}{\gamma}\Big\}\Big]$
	g_0	$g(0)$	$\tilde{g}_0$	$g_0\sqrt{1-\gamma^2}$
	w_c	$1/\sqrt{g(0)k(0)}$	$\tilde{w}_c$	$w_c/\sqrt[4]{1-\gamma^2}$
(III) Raised-Cosine Taper	$\varrho(z)$	$\dfrac{1+a\cos bz}{1+a}$	$\tilde{\varrho}(z)$	$\sqrt{\dfrac{(1+a\cos bz)^2-(1+a)^2\gamma^2}{(1+a)^2(1-\gamma^2)}}$
	$u(z)$	$\dfrac{-a(1+a)b\sin bz}{2g_0(1+a\cos bz)^2}$	$\tilde{u}(z)$	$-\dfrac{a(1+a)b(1+a\cos bz)\sin bz}{2g_0[(1+a\cos bz)^2-(1+a)^2\gamma^2]^{3/2}}$
	θ	$\dfrac{z+\frac{a}{b}\sin bz}{1+a}$	$\tilde{\theta}$	$\dfrac{1}{\sqrt{1-\gamma^2}}\Big[(z+\frac{a}{b}\sin bz)/(1+a)-\dfrac{(1+a)\gamma^2}{2b\sqrt{1-a^2}}\mathrm{Sin}^{-1}\Big(\dfrac{\sqrt{1-a^2}\sin bz}{1+a\cos bz}\Big)\Big]$ where $0\leq\lvert a\rvert<1$, $\lvert(1+a)\gamma/(1+a\cos bz)\rvert^2\ll 1$
	g_0	$g(0)$	$\tilde{g}_0$	$g_0\sqrt{1-\gamma^2}$
	w_c	$1/\sqrt{g(0)k(0)}$	$\tilde{w}_c$	$w_c/\sqrt[4]{1-\gamma^2}$

Note: It is assumed that $2\lvert u(z)\rvert \ll 1$ and $2\lvert\tilde{u}(z)\rvert \ll 1$.

$$\tilde{\delta}(z) = \left(\frac{1-\gamma^2}{(az+1)^2-\gamma^2}\right)^{1/4}\left[\left(\delta(0)-\frac{1}{\tilde{g}_0{}^2R}\right)\cos\tilde{g}_0\tilde{\theta} + \left\{\frac{a}{2\tilde{g}_0(1-\gamma^2)}\left(\delta(0)-\frac{1}{\tilde{g}_0{}^2R}\right) + \frac{1}{\tilde{g}_0}\left(\delta'(0)+\frac{2a}{\tilde{g}_0{}^2R}\right)\right\}\sin\tilde{g}_0\tilde{\theta}\right] + \frac{1-\gamma^2}{\tilde{g}_0{}^2R\{(az+1)^2-\gamma^2\}} \tag{36}$$

$$\tilde{w}(z) = \frac{w(0)(1-\gamma^2)^{1/4}}{[(az+1)^2-\gamma^2]^{1/4}}\left[\frac{1}{2}\left\{1+\frac{\tilde{w}_c{}^4}{\lvert S(0)\rvert^4} + \left(1-\frac{\tilde{w}_c{}^4}{\lvert S(0)\rvert^4}\right)\cos 2\tilde{g}_0\tilde{\theta} + \frac{a\sin 2\tilde{g}_0\tilde{\theta}}{g_0(1-\gamma^2)^{3/2}} + \frac{a^2(1-\cos 2\tilde{g}_0\tilde{\theta})}{4g_0{}^2(1-\gamma^2)^3}\right\} + \left\{\frac{a(1-\cos 2\tilde{g}_0\tilde{\theta})}{2g_0(1-\gamma^2)^{3/2}} + \sin 2\tilde{g}_0\tilde{\theta}\right\}\cdot\mathrm{Im}\left\{\frac{\tilde{w}_c{}^2}{S^2(0)}\right\}\right]^{1/2} \tag{37}$$

where

$$\gamma = \sqrt{2}/(g_0R). \tag{38}$$

If the input wavefront coefficient $1/S^2(0)$ is equal to $1/w_c{}^2$, the spot size in the straight section becomes, from (35),

$$w(z) = \frac{w_c}{(az+1)^{1/2}}\left\{1+\frac{a}{2g_0}\sin 2g_0\theta + \frac{a^2}{8g_0{}^2}(1-\cos 2g_0\theta)\right\}^{1/2}. \tag{39}$$

It is seen from (39) that for the case where the medium is not tapered ($a = 0$) the spot size keeps a constant value for the input beam with $S(0) = w_c$, while for the case of the tapered medium ($a \neq 0$) it fluctuates due to the terms $\sin 2g_0\theta$ and $\cos 2g_0\theta$. In order to eliminate the fluctuation, it is sufficient to choose the input wavefront coefficient as

$$\frac{1}{S^2(0)} = \frac{1}{w_c{}^2} - j\frac{a}{2g_0w_c{}^2}. \tag{40}$$

In this case we have the spot size as

$$w(z) = w_c/(az+1)^{1/2} \tag{41}$$

which does not fluctuate anymore, decreasing (for $a > 0$) or increasing (for $a < 0$) monotonically.

Similarly, if we choose the input wavefront coefficient as

$$\frac{1}{\tilde{S}^2(0)} = \frac{(1-\gamma^2)^{1/2}}{w_c{}^2} - j\frac{a(1-\gamma^2)^{1/2}}{2g_0w_c{}^2} \tag{42}$$

we get the corresponding spot size for the circularly bent section as

$$\tilde{w}(z) = w_c/[(az+1)^2-\gamma^2]^{1/4}. \tag{43}$$

Fig. 2(a) illustrates the calculated spot size in the straight section $w(z)$ normalized by the input value $w(0)$ as a function of the normalized distance z/a^{-1}. The parameter $a/2g_0$ and the input wavefront coefficient $1/S^2(0)$ are taken as $a/2g_0 = 0.05$ and $1/S^2(0) = 1/4w_c{}^2$, $1/w_c{}^2$, and $4/w_c{}^2$. Fig. 2(b) shows the calculated trajectory of the beam center in the straight section normalized by the input value $\delta(0)$, as a function of z/a^{-1}, for the parameters $a/2g_0 = 0.05$ and $\delta'(0) = 0$. It can be seen from these figures that the light beam propagates with fluctuations in both the spot size and the beam trajectory, decreasing the amplitudes and periods of the undulations. It can also be seen that if the input displacement of the beam center and its slope are zero (i.e., $\delta(0) = \delta'(0) = 0$) and the input wavefront coefficient $1/S^2(0)$ is given by (40), the fluctuations are completely removed.

Fig. 3 illustrates the calculated trajectory of the beam center in the circularly bent section. In this figure the parameters are chosen to be $a/2\tilde{g}_0 = 0.05$, $\tilde{g}_0R\cdot\delta(0) = 0.6$, and $\tilde{g}_0R\delta'(0) = 0.12$. The beam trajectory in the circular bend undulates with decreasing amplitude and period, and asymptotically approaches the center axis of

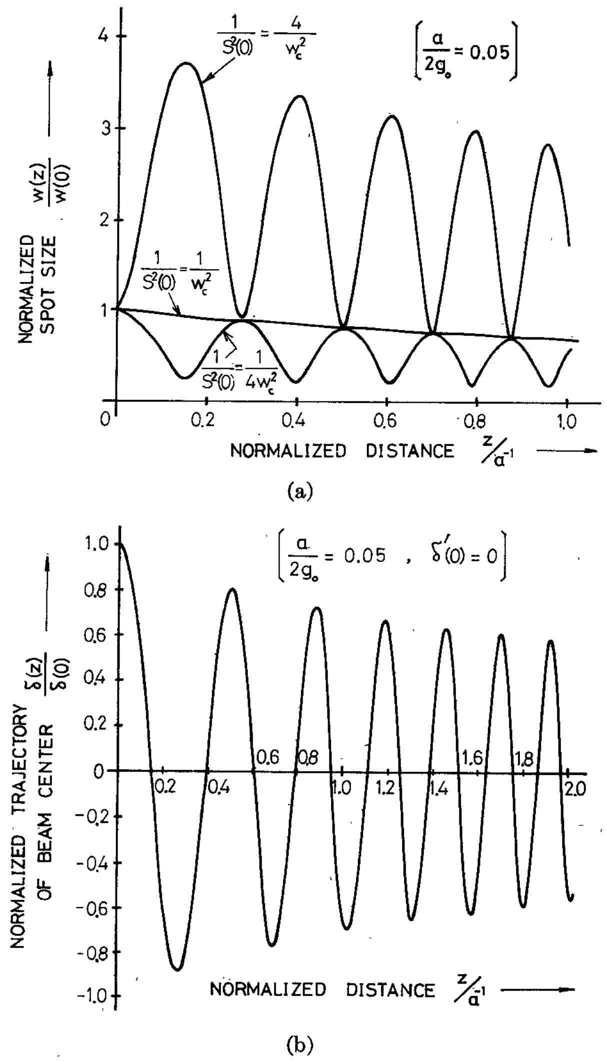

Fig. 2. Calculated spot sizes and trajectory of beam center of the light beam in the straight section of the first kind of tapered lenslike medium with a linear taper.

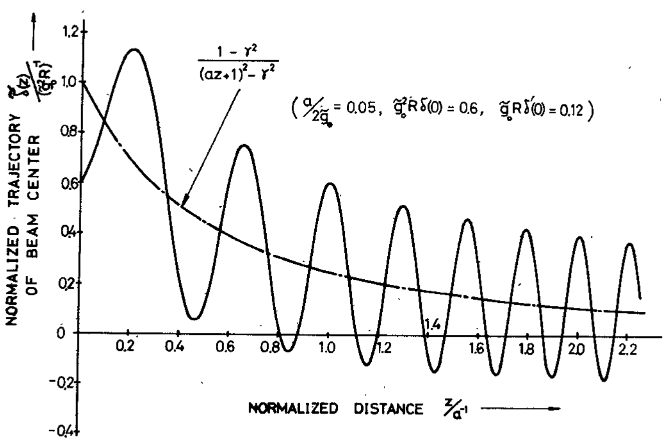

Fig. 3. Calculated trajectory of beam center of the light beam in the circularly bent section of the first kind of tapered lenslike medium with a linear taper.

the medium ($r = R$). Particularly, if we choose the input displacement of the beam center and its slope to be

$$\delta(0) = \frac{1}{\tilde{g}_0^2 R} \quad \delta'(0) = -\frac{2a}{\tilde{g}_0^2 R} \tag{44}$$

then the beam trajectory becomes

$$\tilde{\delta}(z) = \frac{1-\gamma^2}{\tilde{g}_0^2\{(az+1)^2-\gamma^2\}R}. \tag{45}$$

In this case the beam trajectory no longer undulates. Moreover, if the input wavefront coefficient is selected as that given by (42), the spot size does not fluctuate either.

2) Exponential Taper: Let us investigate the behavior of light beams along an exponential taper in which the functions defining the shape of taper are given by

$$G(z) = 1 \quad g(z) = g_0 \exp[az] \tag{46}$$

where a is a constant, and $g_0 > 0$.

The field distribution function $U(x,z)$ for the input beam given by (7) can be obtained by substituting into (31) $\rho(z) \sim w_c$ in (II) of Table II for the straight section and $\tilde{\rho}(z) \sim \tilde{w}_c$ in (II) of that table for the circularly bent section. Further, the trajectory of the beam center and the spot size can be derived by substituting $\rho(z) \sim w_c$ or $\tilde{\rho}(z) \sim \tilde{w}_c$ in (II) of the same table into the corresponding expressions given in Table I.

From the results we see that the light beam propagates with undulating beam trajectory and fluctuating spot size, decreasing ($a > 0$) or increasing ($a < 0$) the amplitudes and periods of the undulations or fluctuations. The undulations or fluctuations can be removed under the same conditions as in the case of the linear taper. If $\delta(0) = \delta'(0) = 0$ and (40) holds, the beam trajectory and the spot size in the straight section are expressed as

$$\delta(z) = 0$$
$$w(z) = w_c \exp[-az/2] \tag{47}$$

and if (42) and (44) are satisfied, they become in the circular bend

$$\tilde{\delta}(z) = \frac{1-\gamma^2}{\tilde{g}_0^2\{\exp[2az]-\gamma^2\}R}$$
$$\tilde{w}(z) = w_c/\{\exp[2az]-\gamma^2\}^{1/4}. \tag{48}$$

3) Raised-Cosine Taper: Let us consider the case where $G(z) = 1$ and the function $g(z)$ is given by a raised-cosine function in the form

$$g(z) = \frac{g_0}{1+a}(1 + a\cos bz) \tag{49}$$

where g_0, a, and b are constants, and it is assumed that $0 < |a| < 1$ and $b > 0$.

The field distribution function $U(x,z)$ for the input beam of (7) is derived by substituting into (31) $\rho(z) \sim w_c$ or $\tilde{\rho}(z) \sim \tilde{w}_c$ in (III) of Table II for the straight or circularly bent sections, correspondingly. It can be seen from these results that the beam trajectory and the spot size undulate in the raised-cosined tapered medium as well. The input conditions to remove the undulations of the light beam are given for the straight section as

$$\delta(0) = \delta'(0) = 0 \quad \frac{1}{S^2(0)} = \frac{1}{w_c^2} \tag{50}$$

and for the circularly bent section as

$$\delta(0) = 1/\tilde{g}_0{}^2R \quad \delta'(0) = 0$$
$$1/\tilde{S}^2(0) = (1-\gamma^2)^{1/2}/w_c{}^2. \qquad (51)$$

The beam trajectory and the spot size corresponding to the input conditions of (50) and (51) are, for the straight section,

$$\delta(z) = 0$$
$$w(z) = w_c(1+a)^{1/2}/(1+a\cos bz)^{1/2} \qquad (52)$$

and for the circularly bent section

$$\tilde{\delta}(z) = (1+a)^2/\{\tilde{g}_0{}^2R(1+a\cos bz)^2\}$$
$$\tilde{w}(z) = w_c/[(1+a\cos bz)^2/(1+a)^2 - \gamma^2]^{1/4}. \qquad (53)$$

It must be noted that the input wavefront coefficients to eliminate the fluctuation of spot size are complex values as given by (40) and (42) for the linear and exponential tapers, whereas for the raised-cosine taper they are real values as given by (50) and (51).

B. Tapered Lenslike Medium of the Second Kind

Next we consider the case that $G(z)$ and $g(z)$ are related by

$$g^2(z) - \sigma'(z) - \sigma^2(z) = \Gamma^2 \quad (= \text{constant}). \qquad (54)$$

In this case, (13) can be solved exactly and has the oscillatory, nonoscillatory, and critically damped solutions corresponding to $\Gamma^2 > 0$, $\Gamma^2 < 0$, and $\Gamma^2 = 0$. As a result, the wavefront coefficient $1/S^2(z)$, the trajectory of the beam center $\delta(z)$ and its slope $\delta'(z)$, and the spot size of the Gaussian beam $w(z)$ are calculated for the straight section, as shown in Table III.

The functions $G(z)$ and $g(z)$, which satisfy the relation of (54), cannot be determined uniquely. As an example, let us consider the simplest case where $g(z) = g$ (= a positive constant) and $G(z) = \exp[2\alpha z]$ (α = a positive constant). Then we have for the straight section

$$\Gamma^2 = g^2 - \alpha^2. \qquad (55)$$

Thus, in this case, we obtain oscillatory, nonoscillatory, and critically damped responses of the light beam, respectively, according to $g^2 > \alpha^2$, $g^2 < \alpha^2$, and $g^2 = \alpha^2$. Figs. 4 and 5 show the calculated trajectories of the beam center $\delta(z)$ and their slopes $\delta'(z)$ normalized by the input value $\delta(0)$, and the calculated spot sizes $w(z)$ normalized by the input spot size $w(0)$, as a function of the normalized distance $z/\Gamma_0{}^{-1}$. The material constant α/g and the input conditions of the light beam $\delta(0)$, $\delta'(0)$, and $w(0)$ used for the numerical calculations are given in these figures. From Figs. 4 and 5, it is seen that for the case of $g > \alpha$ the light beam exhibits oscillatory responses; and the undulating beam trajectory and its slope, as well as the spot size, decrease in amplitude with increasing the propagation distance z. On the other hand, for the case of $g \leq \alpha$ the oscillatory responses disappear and the light beam shows uniformly focusing response in the propagation direction. Especially for the critical case of $g = \alpha$, the most remarkable focusing effect is obtained, i.e., the light beam is focused onto the transmission axis with the shortest distance from $z = 0$.

We can explain the preceding three kinds of response of the light beam qualitatively as follows.

For convenience, let us define two domains D_x and D_z, as shown in Table IV, according to the differences of the permittivity distribution in the x and z directions. That is to say, D_x is the domain in which the distribution of the permittivity is such that the rate of decrease in the x direction is greater than the rate of increase in the z direction, while domain D_z is such that the rate of increase in the z direction is greater than the rate of decrease in the x direction. In Table IV, $P(x_P,z_P)$ and $Q(x_Q,z_Q)$ are any two given points in the respective domains, and $\epsilon(P)$ and $\epsilon(Q)$ represent the permittivities of the points P and Q, respectively. Further, $v(P)$ and $v(Q)$ denote the propagation velocities of the light wave at the respective points.

First, let us consider the oscillatory case of $g > \alpha$ (the general case where $\Gamma^2 > 0$). In this case we can consider that the previously defined domains D_x and D_z have such a distribution as shown in Fig. 6(a), i.e., the domain D_x occupies a great part of the medium and the domain D_z is limited to the z axis and its vicinity. In the domain D_x the permittivity is large near the z axis, and hence the propagation velocity of the light beam will be faster away from the z axis. As a result, the light beam as a whole will be bent along the path $C_1 \rightarrow C_2 \rightarrow C_3 \rightarrow \cdots$, as shown in Fig. 7(a), and thus propagate in undulating fashion. When the light beam passes through the domain D_z, in which the permittivity takes greater values for large values of z, the propagation velocity of the light beam will become slower in the side away from the x axis. Consequently, the light beam will be pulled toward the z axis as it crosses the z axis in the upper or lower right-hand direction. Thus the undulating trajectory of the light beam will decrease in amplitude with increase of propagation distance.

Next we consider the nonoscillatory and the critical cases where $g \leq \alpha$ (the general cases $\Gamma^2 \leq 0$). For these cases the distribution of the domains D_x and D_z is illustrated as in Fig. 6(b). Thus in the domain D_x the propagation velocity of the light beam will be faster in the side away from the z axis and will be slower in the side near the axis. As a result, the light beam as a whole will be bent along the path $C_1 \rightarrow C_2 \rightarrow C_3 \rightarrow \cdots$ and enter the domain D_z as shown in Fig. 7(b). Then, as stated before, in the domain D_z the propagation velocity of the light beam is slower in the side away from the x axis, the light beam as a whole will be bent along the path $C_4 \rightarrow C_5 \rightarrow C_6 \rightarrow \cdots$, and asymptotically approach the z axis without undulation. In this case the speed of asymptotic approach of the light beam to the z axis depends on the values of the permittivities $\epsilon(P_i)$ and $\epsilon(Q_i)$. Therefore with a certain permittivity distribution the trajectory of the light beam will approach the z axis most rapidly, i.e., the optimum focusing effect will be obtained. Accordingly, the critical case of $g = \alpha$ (the general case of $\Gamma^2 = 0$) can be considered to represent such an optimum response.

In the preceding we have explained qualitatively only

TABLE III
PRIMARY PARAMETERS GOVERNING THE PROPAGATION BEHAVIOR OF LIGHT BEAMS ALONG THE TAPERED LENSLIKE MEDIUM OF THE SECOND KIND

(I) Oscillatory Case $\Gamma^2 > 0$	$\frac{1}{S_1^2(Z)} - \frac{h(Z)}{S^2(0)} \cdot \frac{\cos\beta Z - U_1(Z)\sin\beta Z - j\frac{S^2(0)}{W_1^2}\left[\{1+U_1(0)U_1(Z)\}\sin\beta Z + \{U_1(Z)-U_1(0)\}\cos\beta Z\right]}{\cos\beta Z + U_1(0)\sin\beta Z - j\frac{W_1^2}{S(0)}\sin\beta Z}$ $\delta_1(Z) = h^{-1/2}(Z)\left[\delta(0)\{\cos\beta Z + U_1(0)\sin\beta Z\} + \frac{\delta'(0)}{\beta}\sin\beta Z\right]$ $\delta_1'(Z) = -h^{-1/2}(Z)\left[\!\left[\delta(0)\beta\left[\{1+U_1(0)U_1(Z)\}\sin\beta Z + \{U_1(Z)-U_1(0)\}\cos\beta Z\right] + \delta'(0)\{U_1(Z)\sin\beta Z - \cos\beta Z\}\right]\!\right]$ $W_1(Z) = \left[\!\left[\frac{1}{2}\left[1+U_1^2(0)+\left\|\frac{W_1}{S(0)}\right\|^4 + \left\{1-U_1^2(0)-\left\|\frac{W_1}{S(0)}\right\|^4\right\}\cos 2\beta Z + 2U_1(0)\sin 2\beta Z\right] + \{U_1(0)(1-\cos 2\beta Z) + \sin 2\beta Z\}\cdot \mathrm{Im}\left\{\frac{W_1^2}{S^2(0)}\right\}\right]\!\right]^{1/2} \Big/ \left[\frac{h(Z)}{W_1^2}\cdot \mathrm{Re}\left\{\frac{W_1^2}{S^2(0)}\right\}\right]^{1/2}$ where $\beta = \sqrt{g^2(Z) - \sigma^2(Z) - \sigma'(Z)}$, $W_1 = 1\big/\sqrt{\beta k(0) G(0)}$, $h(Z) = \frac{G(Z)}{G(0)}$, $U_1(Z) = \frac{h'(Z)}{2\beta h(Z)}$
(II) Non-Oscillatory Case $\Gamma^2 < 0$	$\frac{1}{S_2^2(Z)} = \frac{h(Z)}{S^2(0)} \cdot \frac{\cosh\bar{\gamma} Z - U_2(Z)\sinh\bar{\gamma} Z + j\frac{S^2(0)}{W_2^2}\left[\{1-U_2(0)U_2(Z)\}\sinh\bar{\gamma} Z - \{U_2(Z)-U_2(0)\}\cosh\bar{\gamma} Z\right]}{\cosh\bar{\gamma} Z + U_2(0)\sinh\bar{\gamma} Z - j\frac{W_2^2}{S^2(0)}\sinh\bar{\gamma} Z}$ $\delta_2(Z) = h^{-1/2}(Z)\left[\delta(0)\{\cosh\bar{\gamma} Z + U_2(0)\sinh\bar{\gamma} Z\} + \frac{\delta'(0)}{\bar{\gamma}}\sinh\bar{\gamma} Z\right]$ $\delta_2'(Z) = h^{-1/2}(Z)\left[\delta(0)\bar{\gamma}\left[\{1-U_2(0)U_2(Z)\}\sinh\bar{\gamma} Z - \{U_2(Z)-U_2(0)\}\cosh\bar{\gamma} Z\right] - \delta'(0)\{U_2(Z)\sinh\bar{\gamma} Z - \cosh\bar{\gamma} Z\}\right]$ $W_2(Z) = \left[\!\left[\frac{1}{2}\left[1-U_2^2(0)-\left\|\frac{W_2}{S(0)}\right\|^4 + \left\{1+U_2^2(0)+\left\|\frac{W_2}{S(0)}\right\|^4\right\}\cosh 2\bar{\gamma} Z + 2U_2(0)\sinh 2\bar{\gamma} Z\right] + \{U_2(0)(\cosh 2\bar{\gamma} Z - 1) + \sinh 2\bar{\gamma} Z\}\, \mathrm{Im}\left\{\frac{W_2^2}{S^2(0)}\right\}\right]\!\right]^{1/2} \Big/ \left[\frac{h(Z)}{W_2^2}\cdot \mathrm{Re}\left\{\frac{W_2^2}{S^2(0)}\right\}\right]^{1/2}$ where $\bar{\gamma} = \sqrt{\sigma^2(Z) + \sigma'(Z) - g^2(Z)}$, $W_2 = 1\big/\sqrt{\bar{\gamma} k(0) G(0)}$, $h(Z) = \frac{G(Z)}{G(0)}$, $U_2(Z) = \frac{h'(Z)}{2\bar{\gamma} h(Z)}$
(III) Critical Case $\Gamma^2 = 0$	$\frac{1}{S_3^2(Z)} = \frac{h(Z)}{S^2(0)} \cdot \frac{1 - U_3(Z)g(0)Z - j\frac{S^2(0)}{W_3^2}\{U_3(0)U_3(Z)g(0)Z + U_3(Z) - U_3(0)\}}{1 + U_3(0)g(0)Z - j\frac{W_3^2}{S^2(0)}g(0)Z}$ $\delta_3(Z) = h^{-1/2}(Z)\left[\delta(0) + \left\{U_3(0)\delta(0) + \frac{\delta'(0)}{g(0)}\right\}g(0)Z\right]$ $\delta_3'(Z) = -g(0)h^{-1/2}(Z)\left[U_3(Z)\left\{U_3(0)\delta(0) + \frac{\delta'(0)}{g(0)}\right\}g(0)Z + \delta(0)\{U_3(Z)-U_3(0)\} - \frac{\delta'(0)}{g(0)}\right]$ $W_3(Z) = \left[1 + 2U_3(0)g(0)Z + \left\{U_3^2(0) + \left\|\frac{W_3}{S(0)}\right\|^4\right\}g^2(0)Z^2 + 2g(0)Z\{1+U_3(0)g(0)Z\} \cdot \mathrm{Im}\left\{\frac{W_3^2}{S^2(0)}\right\}\right]^{1/2} \Big/ \left[\frac{h(Z)}{W_3^2}\cdot \mathrm{Re}\left\{\frac{W_3^2}{S^2(0)}\right\}\right]^{1/2}$ where $g(Z) = \sqrt{\sigma'(Z) + \sigma^2(Z)}$, $W_3 = 1\big/\sqrt{k(0)g(0)G(0)}$, $h(Z) = \frac{G(Z)}{G(0)}$, $U_3(Z) = \frac{h'(Z)}{2g(0)h(Z)}$

Note: The parameters $G(z)$ and $g(z)$ have a fixed relation as $g^2(z) - \sigma'(z) - \sigma^2(z) = \Gamma^2 =$ constant.

the variation of the trajectory of the beam center. Similar qualitative explanation is possible for the variation of the spot sizes as shown in Fig. 5.

C. Comparison of the Two Kinds of Tapered Lenslike Media

From (33)–(35) obtained for the linearly tapered lenslike medium, we see that for the positive values of the taper constant ($a > 0$) the undulating amplitude of the spot size $w(z)$ and the trajectory of the beam center $\delta(z)$ decrease with increasing the transmission distance z, while the slope of the beam trajectory $\delta'(z)$ increases. Although these results are obtained for the restricted case in which the permittivity profile is given by $\epsilon(x,z) = \epsilon(0)\{1 - g_0^2(az+1)^2x^2\}$, examination of the expressions for $w(z)$, $\delta(z)$, and $\delta'(z)$ given in Table I shows that similar results will be obtained for more general cases in which only the focusing parameter $g(z)$ has a gradient in the axial direction. That is to say, in the prototype of the first kind of tapered lenslike medium, the undulation of the slope of

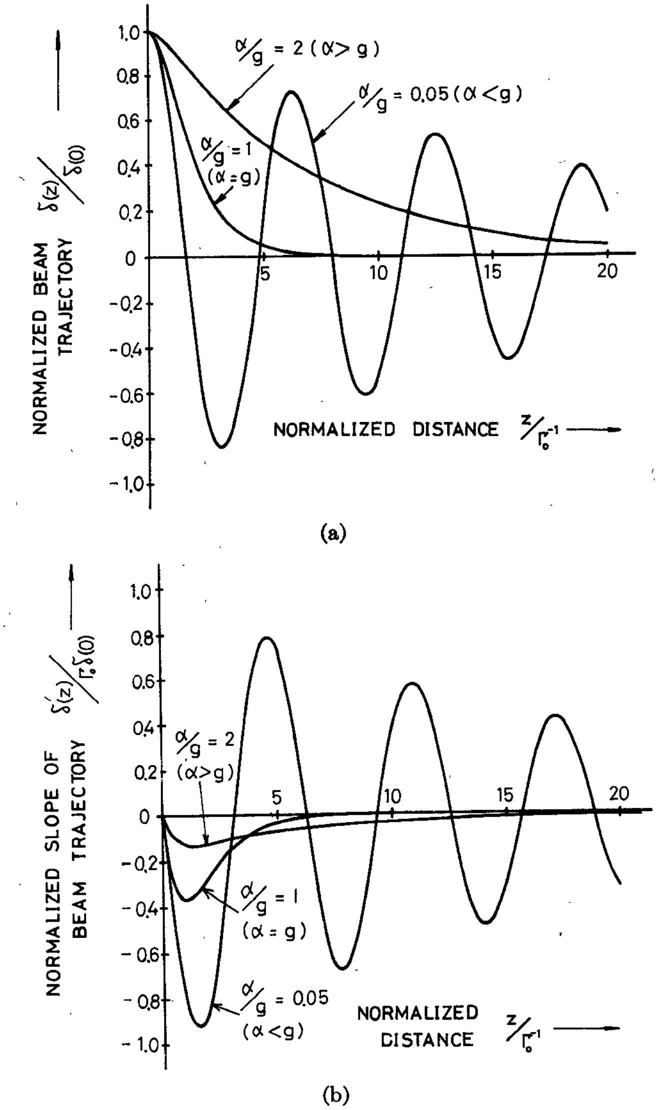

Fig. 4. Calculated trajectories and slopes of beam center of the light beam guided along the second kind of tapered lenslike medium whose permittivity is given by $\epsilon(x,z) = \epsilon(0) \exp[2\alpha z](1 - g^2x^2)$. Γ_0 represents β, $\overline{\gamma}$, and g in accordance with $\alpha^2 < g^2$, $\alpha^2 > g^2$, and $\alpha^2 = g^2$, respectively ($\delta(0) \neq 0$, $\delta'(0) = 0$). (a) Beam trajectories. (b) Slope of beam trajectories. (It is assumed that $\alpha > 0$ and $g > 0$.)

the beam trajectory $\delta'(z)$ increases in amplitude if the functional form of the taper for the focusing parameter $g(z)$ is selected such that the undulations of the beam trajectory $\delta(z)$ and the spot size $w(z)$ decrease in amplitude.

On the other hand, in the second kind of tapered lenslike medium, we see from the expressions given in (I) of Table III that the undulating amplitudes of $\delta'(z)$, as well as $\delta(z)$ and $w(z)$, can be reduced regardless of the incidence conditions if the functional forms of the tapers for the permittivity profile and focusing parameter, $G(z)$ and $g(z)$, are selected such that they satisfy the relation of (54) and $G(z)$ is an increasing function of z.

Further, the second kind of tapered lenslike medium possesses the following other interesting properties which are not found in the prototype of the first kind of tapered lenslike medium. The light beam exhibits three types of responses—oscillatory, nonoscillatory, and critically

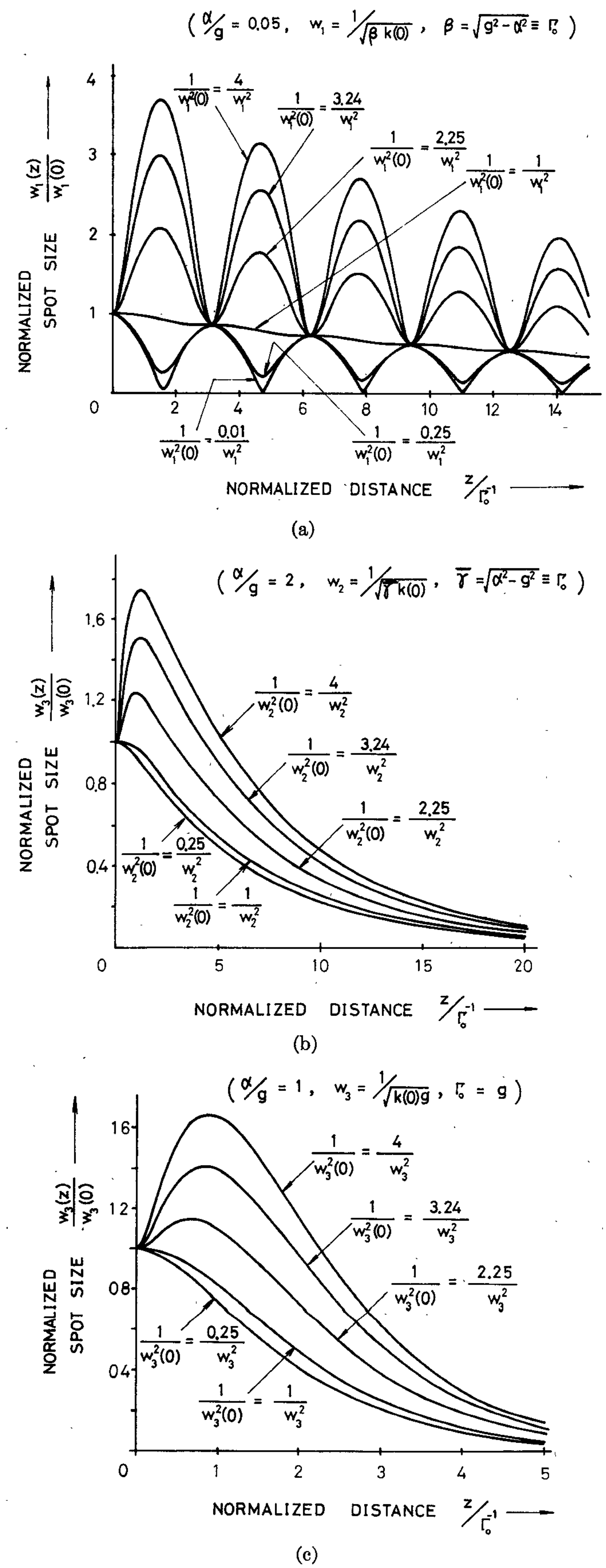

Fig. 5. Calculated spot sizes of the light beam guided along the second kind of tapered lenslike medium whose permittivity is given by $\epsilon(x,z) = \epsilon(0) \exp[2\alpha z](1 - g^2x^2)$. (a) Oscillatory case ($\alpha^2 < g^2$). (b) Nonoscillatory case ($\alpha^2 > g^2$). (c) Critically damped case ($\alpha^2 = g^2$). (It is assumed that $\alpha > 0$ and $g > 0$.)

TABLE IV
Two Domains D_x and D_z Classified by the Difference of Permittivity Distribution in the x and z Directions

Domain	Coordinates of Points P and Q: Coordinate x	Coordinates of Points P and Q: Coordinate z	Permittivities at Points P and Q	Propagation Velocity at Points P, Q
D_x	$\lvert X_P \rvert < \lvert X_Q \rvert$	arbitrary	$\varepsilon(P) > \varepsilon(Q)$	$\lvert V(P) \rvert < \lvert V(Q) \rvert$
	$\lvert X_P \rvert = \lvert X_Q \rvert$	$Z_P \leq Z_Q$	$\varepsilon(P) \leq \varepsilon(Q)$	$\lvert V(P) \rvert \geq \lvert V(Q) \rvert$
D_z	arbitrary	$Z_P > Z_Q$	$\varepsilon(P) > \varepsilon(Q)$	$\lvert V(P) \rvert < \lvert V(Q) \rvert$
	$\lvert X_P \rvert \leq \lvert X_Q \rvert$	$Z_P = Z_Q$	$\varepsilon(P) \geq \varepsilon(Q)$	$\lvert V(P) \rvert \leq \lvert V(Q) \rvert$

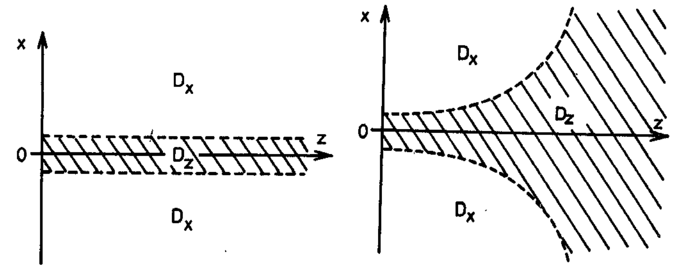

Fig. 6. Illustrative diagram (I) for explaining qualitatively (a) oscillatory and (b) nonoscillatory and critically damped responses of the light beam.

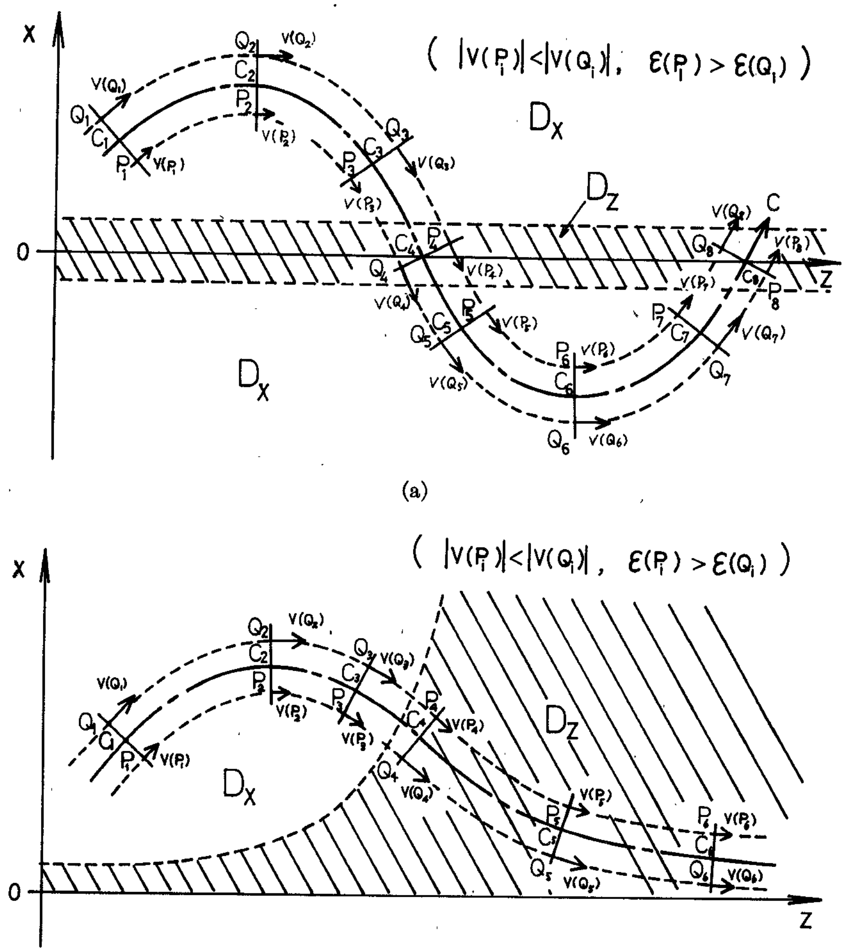

(b)

Fig. 7. Illustrative diagram (II) for explaining qualitatively oscillatory, nonoscillatory, and critically damped responses of the light beam. (a) Oscillatory case ($\alpha^2 < g^2$: $\Gamma^2 > 0$). (b) Nonoscillatory and critically damped cases ($\alpha^2 \geq g^2$: $\Gamma^2 \leq 0$).

damped responses—according to the differences of the axial gradient given to the focusing parameter and the on-axis permittivity. Especially if we select $g(z)$ and $G(z)$ as

$$g(z) = [\sigma^2(z) + \sigma'(z)]^{1/2}$$

$$G(z) = K_0 \exp\left[2 \int_0^z \sigma(z)\, dz\right] \tag{56}$$

with

$$G'(z) > 0 \tag{57}$$

by setting the arbitrary constant Γ of (54) as zero, we can completely remove the undulations of the light beam and obtain the optimum focusing effect. In the foregoing expression (56), $\sigma(z)$ is an arbitrary continuous function of z and K_0 is a constant independent of z.

IV. MATCHED WAVEFRONT COEFFICIENTS

In the preceding section the input wavefront coefficients to eliminate the fluctuations of spot sizes in the straight and circularly bent sections have been derived for both the linear and exponential tapers as (40) and (42), and for the raised-cosine taper as (50) and (51). Generally, the corresponding input wavefront coefficients for the first kind of tapered lenslike media can also be derived from the expressions for $1/S^2(z)$ and $1/\tilde{S}^2(z)$ given in Table I. The results are expressed as

$$\frac{1}{S^2(0)} = \frac{1}{w_c^2}\{1 - ju(0)\} \tag{58}$$

$$\frac{1}{\tilde{S}^2(0)} = \frac{1}{\tilde{w}_c^2}\{1 - j\tilde{u}(0)\}. \tag{59}$$

For the input wavefront coefficients of (58) and (59), the spot sizes $w(z), \tilde{w}(z)$ and the wavefront coefficients $1/S^2(z), 1/\tilde{S}^2(z)$ are simplified from the expressions in Table I, respectively, to

$$w(z) = w_c/[\rho(z)]^{1/2} \tag{60}$$

$$\frac{1}{S^2(z)} = \frac{\rho(z)}{w_c^2}\{1 - ju(z)\} \tag{61}$$

and

$$\tilde{w}(z) = \tilde{w}_c/[\tilde{\rho}(z)]^{1/2} \tag{62}$$

$$\frac{1}{\tilde{S}^2(z)} = \frac{\tilde{\rho}(z)}{\tilde{w}_c^2}\{1 - j\tilde{u}(z)\}. \tag{63}$$

From (60)–(63) we see that the fluctuation terms $\cos g_0\theta$ and $\sin g_0\theta$ ($\cos \tilde{g}_0\tilde{\theta}$ and $\sin \tilde{g}_0\tilde{\theta}$) disappear, and hence the fluctuations of the spot sizes in the tapered media are completely eliminated. In this sense we call (58) and (59) the matched input wavefront coefficients, and also (61) and (63) the matched wavefront coefficients for the first kind of tapered lenslike media. Similarly, for the second kind of tapered lenslike media in the oscillatory case ($\Gamma^2 > 0$), the matched input wavefront coefficient, the matched wavefront coefficient, and the corresponding spot size are obtained from (58), (60), and (61) by replacing w_c, $u(0)$, $u(z)$, and $\rho(z)$ with w_1, $u_1(0)$, $u_1(z)$, and $h(z)$ of (I) in Table III for the straight section and with $\tilde{w}_1$, $\tilde{u}_1(0)$, $\tilde{u}_1(z)$, and $h(z)$ for the circularly bent section, in which $\tilde{w}_1$ and $\tilde{u}_1(z)$ are given in the following:

$$\tilde{w}_1 = 1/[\tilde{\beta}\tilde{k}(0)G(0)]^{1/2}$$

$$\tilde{u}_1(z) = \frac{h'(z)}{2\tilde{\beta}h(z)} \tag{64}$$

with

$$\tilde{\beta} = [\tilde{g}^2(z) - \sigma'(z) - \sigma^2(z)]^{1/2}. \tag{65}$$

Application of (61) and (63) to the cases of the linear, exponential, and raised-cosine tapers yields the matched wavefront coefficients as shown in Table V. Fig. 8(a) and (b) shows numerical illustrations of the matched wavefront coefficients in the straight sections for the various tapered lenslike media of the first kind. From the figure we can easily find the matched wavefront coefficients at the entrance ($z = 0$) and exit ($z = l$) planes of the tapered lenslike medium. Especially, we should note that the imaginary part of the matched wavefront coefficient for the exponential taper is constant regardless of the length of the tapered medium l; the shape of phase

TABLE V
MATCHED WAVEFRONT COEFFICIENTS IN THE STRAIGHT AND CIRCULARLY BENT SECTIONS OF THE TAPERED LENSLIKE MEDIUM OF THE FIRST KIND WITH LINEAR, EXPONENTIAL, AND RAISED-COSINE TAPERS

Shape of Taper	Straight Section	Circularly Bent Section
Linear Taper	$\frac{az+1}{w_c^2} - j\frac{a}{2g_0 w_c^2(az+1)}$	$\frac{\sqrt{(az+1)^2-\gamma^2}}{w_c^2} - j\frac{a(az+1)}{2g_0 w_c^2[(az+1)^2-\gamma^2]}$
Exponential Taper	$\frac{e^{az}}{w_c^2} - j\frac{a}{2g_0 w_c^2}$	$\frac{\sqrt{e^{2az}-\gamma^2}}{w_c^2} - j\frac{a e^{2az}}{2g_0 w_c^2(e^{2az}-\gamma^2)}$
Raised-Cosine Taper	$\frac{1+a\cos bz}{w_c^2(1+a)} + j\frac{ab\sin bz}{2g_0 w_c^2(1+a\cos bz)}$	$\frac{\sqrt{(1+a\cos bz)^2-[(1+a)\gamma]^2}}{w_c^2(1+a)} + j\frac{ab(1+a\cos bz)\sin bz}{2g_0 w_c^2[(1+a\cos bz)^2-(1+a)^2\gamma^2]}$

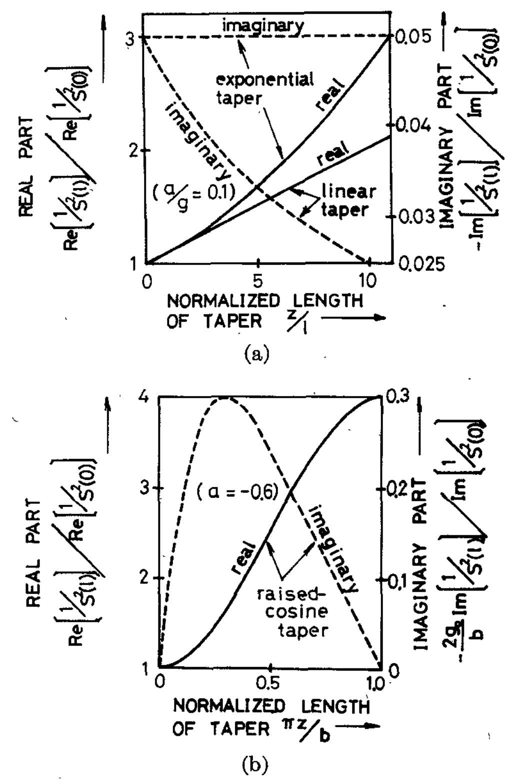

Fig. 8. Numerical illustrations of the matched wavefront coefficients in the straight section of the first kind of tapered lenslike medium (a) for linear and exponential tapers and (b) for raised-cosine taper.

front is conserved against variations of l. Conversely, if we determine the shape of taper in which the imaginary part of the matched wavefront coefficient Im $\{1/S^2(z)\} = -\rho'(z)/2g_0w_c^2\rho(z)$ is independent of z, we find that it is nothing but the exponential taper. Thus we see that the exponential taper possesses an interesting property of conserving the shape of phase front of the light beam with the matched input wavefront coefficient against variations of the length of the tapered medium.

V. APPLICATIONS OF TAPERED LENSLIKE MEDIA

A. Spot-Size Transducer

Suppose that two straight lenslike media with different focusing parameters must be connected. If the two media are connected directly, mode conversion and reconversion occur since the normal modes of the media are different, and, as a result, the spot size of the light beam with input conditions matched to the entrance medium fluctuates in the outgoing medium. If the fluctuation grows remarkably, the diffraction loss due to the finite aperture of the medium increases and also signal distortion arises, deteriorating communication quality. In order to avoid such unfavorable phenomena, we need a matching mechanism between the two media. Certain matching can be done by using the natural focusing properties of multimode sections such as a combination of two or more lenses. In such a mechanism, however, reflection loss due to the abrupt change of the permittivity at the boundaries of the matching lenses would be inevitable, and slight displacement or misadjustment of the lenses would cause appreciable mismatching so that efficient and stable coupling could not always be obtained. In this section we propose a new matching mechanism as shown in Fig. 9, a spot-size transducer composed of a tapered lenslike medium of the first kind, which permits stable and efficient coupling of the two media, and we derive the design conditions for highly efficient coupling.

In order to avoid the fluctuation of the spot size arising from mode conversion and reconversion, we must make both the wavefront coefficients $1/S^2(0)$ at $z = 0$ and $1/S^2(l)$ at $z = l$ equal to the characteristic wavefront coefficients $1/w_{c1}^2$ and $1/w_{c2}^2$ of the media I and II, respectively. That is, we need the following relations:

$$1/S^2(0) = 1/w_{c1}^2$$

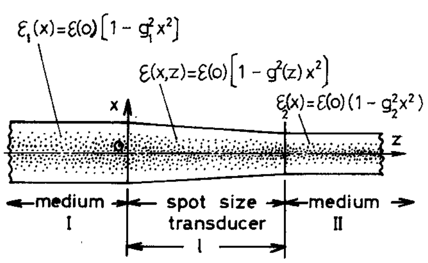

Fig. 9. Spot-size transducer utilizing the first kind of tapered lenslike medium.

$$1/S^2(l) = 1/w_{c2}^2. \quad (66)$$

Let the permittivity of the media I and II be expressed as

$$\epsilon_1(x) = \epsilon(0)(1 - g_1^2x^2)$$
$$\epsilon_2(x) = \epsilon(0)(1 - g_2^2x^2). \quad (67)$$

Then we have

$$1/w_{c1}^2 = g_1k(0)$$
$$1/w_{c2}^2 = g_2k(0). \quad (68)$$

Noticing that both $1/w_{c1}^2$ and $1/w_{c2}^2$ are real values, let us apply the relations of (66) to (61), and we get

$$u(0) = u(l) = 0 \quad (69)$$

$$S^2(0) = w_{c1}^2 = \rho(l)w_{c2}^2. \quad (70)$$

Among the three types of tapered lenslike media investigated in the preceding section, it is only the raised-cosine taper that can satisfy (69) with a finite length of taper l. Set the constant b of (49) as $b = \pi/l$; then (69) is satisfied. Therefore, the following design considerations of the spot-size transducer are limited to the case of using the raised-cosine taper.

The wavefront coefficient of the light beam satisfying the input conditions of (50) is given from Table V as

$$\frac{1}{S^2(z)} = \frac{1 + a\cos bz}{w_c^2(1 + a)} + j\frac{ab\sin bz}{2g_0w_c^2(1 + a\cos bz)}. \quad (71)$$

Substituting (66) and (68) into (71) and setting $b = \pi/l$, we can determine a and g_0 as

$$a = (g_1 - g_2)/(g_1 + g_2) \quad (72)$$

$$g_0 = g_1. \quad (73)$$

Substitution of (66), (72), and (73) in (71) yields the spot size in the transducer as

$$w(z) = w_{c1}\left[\frac{1}{2}\left\{1 + \left(\frac{w_{c1}}{w_{c2}}\right)^2 + \left(1 - \frac{w_{c1}^2}{w_{c2}^2}\right)\cos\frac{\pi z}{l}\right\}\right]^{-1/2}. \quad (74)$$

Moreover, the transfer ratio of the spot size w_{c2}/w_{c1} is calculated from (70) by setting $b = \pi/l$ and $z = l$ of $\rho(z)$ of (III) in Table II as

$$w_{c2}/w_{c1} = \{(1 + a)/(1 - a)\}^{1/2}. \quad (75)$$

Fig. 10(a) illustrates the relationship between w_{c2}/w_{c1} and a given by (75). From this figure we can readily find the approximate value of w_{c2}/w_{c1} as a function of the parameter a involved in (49); for example, if we set $a = -0.6$, we have $w_{c2}/w_{c1} = 0.5$, and hence for this case the light beam at the exit of the transducer $z = l$ has the spot size reduced by half of the input value. Fig. 10(b) displays the normalized spot sizes in the transducer of (74) for the transfer ratios $w_{c2}/w_{c1} = 0.8$, 0.5, and 0.2, as a function of the normalized distance z/l.

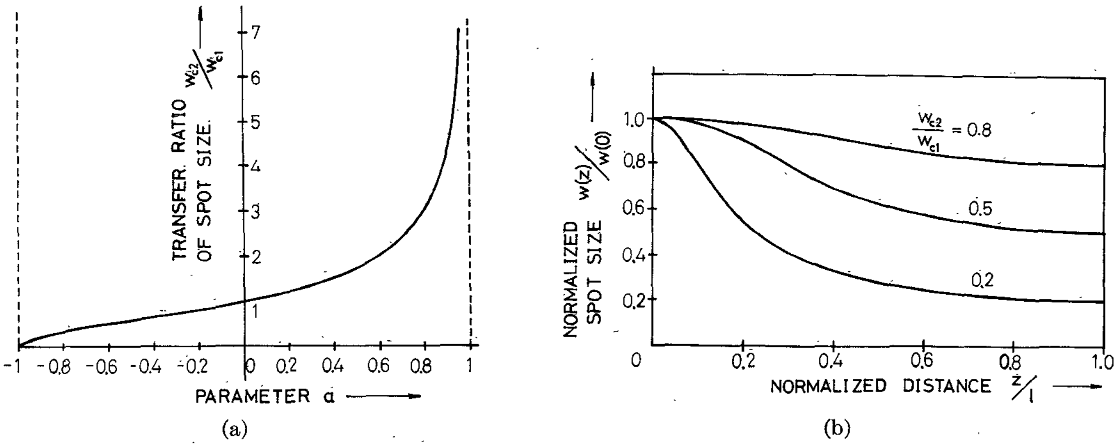

Fig. 10. (a) Transfer ratio of spot size and (b) its variations in a spot-size transducer, utilizing the first kind of tapered lenslike medium with a raised-cosine taper.

B. Mode Transducer for Use in a Circular Bend

Let us suppose that the straight section of an optical fiber consisting of a lenslike medium must be connected to the circularly bent section of that fiber without offsetting and tilting the center axis of the medium. If we connect the two sections directly, the light beam propagating along the circular bend is accompanied with the undulations of the beam trajectory and the fluctuations of the spot size because of the difference of normal modes in each section. These undulations and fluctuations are also unfavorable from the transmission system point of view. Such unfavorable phenomena, however, can be suppressed by inserting a mode transducer between the straight and circularly bent sections, as shown in Fig. 11. The portion $\widehat{OA}$ in the figure represents the mode transducer, which is effective in converting normal modes of the straight section into those of the circularly bent section.

Let the curved lenslike medium with a raised-cosine taper be inserted in the portion $\widehat{OA}$ as the mode transducer. The trajectory of the light beam incident on the circular bend $\widehat{OA}$ along its axis can be obtained by substituting $\tilde{p}(z) \sim \tilde{g}_0$ of (III) in Table II into the expression for $\tilde{\delta}(z)$ given in Table I and setting $\delta(0) = \delta'(0) = 0$ as

$$\tilde{\delta}(z) = -\{J(z) \cos \tilde{g}_0\tilde{\theta} - J^4(z)\}/(\tilde{g}_0^2R) \tag{76}$$

with

$$J(z) = \left(1 - \frac{2}{g_0^2R^2}\right)^{1/4} \left[\left(\frac{1 + a \cos bz}{1 + a}\right)^2 - \frac{2}{g_0^2R^2}\right]^{-1/4}. \tag{77}$$

The parameters $\tilde{g}_0$ and $\tilde{\theta}$ are given in (III) of Table II.

If we take the length of the tapered medium l as

$$l = \pi/b = \pi/\tilde{g}_0 = \pi/\{g_0[1 - 2/(g_0R)^2]^{1/2}\} \tag{78}$$

we get from (76)

$$\tilde{\delta}(l) = \{J^4(l) + J(l)\}/(\tilde{g}_0^2R) \tag{79}$$

$$\tilde{\delta}'(l) = \frac{d}{dz}\tilde{\delta}(z)\bigg|_{l=0} = 0. \tag{80}$$

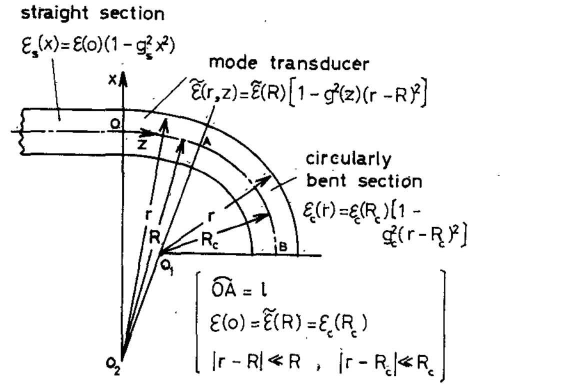

Fig. 11. Mode transducer for use in a circularly bent section of an optical waveguide consisting of lenslike medium.

Accordingly, the condition to eliminate the undulation from the trajectory of the beam center is given as

$$1/\tilde{g}_c^2R = \{J(l) + J^4(l)\}/(\tilde{g}_0^2R) \tag{81}$$

with

$$\tilde{g}_c = g_s[1 - 2/(g_sR_c)^2]^{1/2} \tag{82}$$

where the permittivity profiles are assumed to be for the straight section $\widehat{SO}$

$$\epsilon_s(x) = \epsilon(0)(1 - g_s^2x^2) \tag{83}$$

and for the circularly bent section $\widehat{AB}$

$$\epsilon_c(r) = \epsilon_c(R_c)[1 - g_c^2(r - R_c)^2]. \tag{84}$$

The matching conditions for the characteristic spot sizes at the entrance and exit of the mode transducer are derived from (53) and (78) as follows:

$$w_c\{1 - 2/(g_0R)^2\}^{-1/4} = \tilde{w}_{ci} \; (\equiv 1/[g_sk(0)]^{1/2}) \tag{85}$$

$$w_c\left\{\left(\frac{1 - a}{1 + a}\right)^2 - \frac{2}{g_0^2R^2}\right\}^{-1/4} = \tilde{w}_{c0} \; (\equiv 1/[\tilde{g}_ck(0)]^{1/2}). \tag{86}$$

From (78), (81), (85), and (86), we can determine the parameters g_0, a, b, and R, which are involved in the expression for the permittivity profile of the mode transducer

$$\tilde{\epsilon}(r,z) = \tilde{\epsilon}(R)\{1 - g_0^2(1 + a\cos bz)^2(r - R)^2/(1 + a)^2\}. \quad (87)$$

If we assume $\epsilon_c(R_c) = \epsilon_s(0)$ and $g_c = g_s$, we obtain the following results:

$$R = R_c\{1 + (1 - 2/g_s^2R_c^2)^{3/4}\}$$
$$g_0 = g_s\left(1 + \frac{2}{g_s^2R^2}\right)^{1/2}$$
$$a = \frac{2}{g_0^2R_c^2}\Big/\left[1 + \left(1 - \frac{2}{g_0^2R_c^2}\right)^{1/2}\right]^2$$
$$b = g_0\left(1 - \frac{2}{g_0^2R^2}\right)^{1/2}. \quad (88)$$

The results of (88) represent the design conditions for the mode transducer consisting of a raised-cosine tapered medium.

C. Ray-Oscillation Suppressor

As described in the preceding section, the second kind of tapered lenslike medium possesses an interesting property: the undulating amplitudes of the slope of the beam trajectory $\delta'(z)$, as well as the beam trajectory $\delta(z)$ and the spot size $w(z)$, can be reduced if the functional forms of the tapers $G(z)$ and $g(z)$ are chosen such that (54) is satisfied and $G(z)$ is an increasing function of z.

This property of the second kind of tapered lenslike medium makes it possible to construct an ROS with only a passive medium. According to [12], however, the realization of an ROS with only a passive medium is limited to the case of transmitting a light beam from a region of low to one of high permittivity, which is proved by Liouville's theorem. Accordingly, if we insert such an ROS in the connecting terminals of two light-focusing fibers consisting of lenslike media with different permittivity on the center axis, we can suppress the undulation of the light beam propagating from the fiber of low to one of high permittivity.

Further, if such an ROS is installed in the photoreceiving terminal plane of a photodetector such as an avalanche photodiode or a photomultiplier, it acts as a component not only to enlarge the light-receiving area but also to increase the light-acceptance angle.

VI. CONCLUSION

In the present paper we have derived general expressions for the response of the electromagnetic fields in the tapered lenslike medium on the basis of the approximate wave theory, which were not obtained in the previous papers based on the ray theory. Applying the results to the various tapers, we have investigated the propagation behavior of light beams in detail, theoretically and numerically. As a result, we have clarified that tapered lenslike media can be classified into the first and second kinds, according to the differences of the focusing property. We have also clarified the matching incidence conditions to eliminate the fluctuations of the light beam, which have not yet been obtained in the previous papers.

As an application of the theory, a spot-size transducer and a mode transducer for use in a circular bend have been proposed, which are composed of the first kind of tapered lenslike medium with a raised-cosine taper, and the design conditions for both transducers have been derived. Further, an ROS using the second kind of tapered lenslike medium has been proposed, and its applicability to some new optical circuit components has been discussed.

We have verified that the basic equations for the beam trajectory, the spot size, and the curvature of the phase front obtained in the present paper coincide with those derived from the viewpoint of ray theory, apart from slight differences due to the assumptions introduced for simplification. For the sake of simplicity, we have assumed that the permittivity profile in the transverse cross section is proportional to the square of the distance from the center axis, and also that the material of the medium has no loss and no gain. Furthermore, we have used the TEM wave approximation as well as the paraxial beam approximation. Accordingly, we cannot apply the results of this paper to cases where these approximations are not applicable or satisfied.

APPENDIX
SOLUTION OF THE PARAXIAL WAVE EQUATION (5)

In order to clarify the behavior of the light beam with Hermite–Gaussian transverse field distribution, let us express the field distribution function as [7]–[9]

$$U(x,z) = \exp[A(z)x^2 + B(z)x + C(z)] \cdot \mathrm{He}_n[D(z)x + F(z)] \quad (A1)$$

where $A(z)$, $B(z)$, $C(z)$, $D(z)$, and $F(z)$ are unknown parameters which are assumed to be functions of z, and $\mathrm{He}_n(\mathrm{x})$ denotes the Hermite polynomial of the nth order, defined as

$$\mathrm{He}_n(\mathrm{x}) = n!\sum_{m=0}^{[n/2]} \frac{(-1)^m(2\mathrm{x})^{n-2m}}{m!(n-2m)!} \quad (A2)$$

with

$$\left[\frac{n}{2}\right] = \begin{cases} \dfrac{n}{2}, & n = 2,4,6,\cdots \\ \dfrac{n-1}{2}, & n = 1,3,5,\cdots. \end{cases} \quad (A3)$$

Substituting (A1) in (5) in the text and eliminating the terms $\mathrm{He}_{n-2}(\mathrm{x})$ by using the recurrence relation

$$2(n-1)\,\mathrm{He}_{n-2}(\mathrm{x}) = 2\mathrm{x}\,\mathrm{He}_{n-1}(\mathrm{x}) - \mathrm{He}_n(\mathrm{x}) \quad (A4)$$

we obtain

$$\{\Lambda_1(z)x^2 + \Lambda_2(z)x + \Lambda_3(z)\}\cdot\mathrm{He}_n[D(z)x + F(z)] + \{\Lambda_4(z)x + \Lambda_5(z)\}\cdot\mathrm{He}_{n-1}[D(z)x + F(z)] = 0 \quad (A5)$$

where $\Lambda_i(z)$ $(i = 1,2,\cdots,5)$ represents functions of z, including $A(z)$, $B(z)$, $\cdots$, $F(z)$ and their first derivatives with respect to z. To determine the unknown parameters $A(z), B(z), \cdots, F(z)$, let us express (A5) as a descending power series in x with the help of (A2) and compare terms with equal powers of x. Then we get the following set of differential equations:

$$j2K(z)\frac{dA(z)}{dz} = 4A^2(z) - g^2(z)K^2(z) \tag{A6a}$$

$$j2K(z)\frac{dB(z)}{dz} = 4A(z)B(z) \tag{A6b}$$

$$j2K(z)\frac{dC(z)}{dz} = B^2(z) + 2A(z) - 2nD^2(z) - jK'(z) \tag{A6c}$$

$$jK(z)\frac{dD(z)}{dz} = D(z)\{2A(z) + D^2(z)\} \tag{A6d}$$

$$jK(z)\frac{dF(z)}{dz} = D(z)\{B(z) + F(z)D(z)\}. \tag{A6e}$$

As a first step, to integrate (A6a) and (A6b), let us write

$$A(z) = -j\frac{K(z)}{2}\frac{1}{\xi(z)}\frac{d\xi(z)}{dz} \tag{A7}$$

$$B(z) = -2A(z)\delta(z) - jK(z)\frac{d\delta(z)}{dz} \tag{A8}$$

in which $\xi(z)$ and $\delta(z)$ are newly introduced unknown parameters, being real-valued functions of z.

Substituting (A7) and (A8) in (A6a) and (A6b), we have

$$\frac{d^2\xi(z)}{dz^2} + \frac{K'(z)}{K(z)}\frac{d\xi(z)}{dz} + g^2(z)\xi(z) = 0 \tag{A9}$$

$$\frac{d^2\delta(z)}{dz_2} + \frac{K'(z)}{K(z)}\frac{d\delta(z)}{dz} + g^2(z)\delta(z) = 0. \tag{A10}$$

If we express $\xi(z)$ and $\delta(z)$ as

$$\xi(z) = M(z)/[K(z)]^{1/2} \quad \delta(z) = N(z)/[K(z)]^{1/2} \tag{A11}$$

and substitute into (A9) and (A10), we find that both the newly introduced functions $M(z)$ and $N(z)$ must satisfy the same differential equation as given by (13) in the text. Let the two independent solutions of (13) be $\lambda_1(z)$ and $\lambda_2(z)$. Then we get from (A11)

$$\xi(z) = \frac{1}{[K(z)]^{1/2}}\{a_1\lambda_1(z) + a_2\lambda_2(z)\} \tag{A12}$$

$$\delta(z) = \frac{1}{[K(z)]^{1/2}}\{b_1\lambda_1(z) + b_2\lambda_2(z)\} \tag{A13}$$

where a_1, a_2, b_1, and b_2 denote integration constants to be determined from the input conditions of the light beam.

Consequently, we find the functional forms of $A(z)$ and $B(z)$ by substituting $\xi(z)$ and $\delta(z)$ from (A12) and (A13) into (A7) and (A8).

Next, to integrate (A6d), substitute (A7) in (A6d), and we have

$$\frac{dD(z)}{dz} + \left[\frac{1}{\xi(z)}\frac{d\xi(z)}{dz}\right]D(z) = \left[-\frac{j}{K(z)}\right]D^3(z). \tag{A14}$$

Equation (A14) is a Bernoulli's differential equation and can be integrated as

$$D(z) = \left[K_1\xi^2(z) + j2\xi^2(z)\int\frac{dz}{K(z)\xi^2(z)}\right]^{-1/2} \tag{A15}$$

where K_1 is an integration constant.

Furthermore, integrating (A6c) and (A6e) and substituting for $A(z)$, $B(z)$, and $D(z)$ from (A7), (A8), and (A15), we obtain

$$C(z) = A(z)\delta^2(z) + j\frac{K(z)}{2}\delta(z)\delta'(z) - n\ln D(z) - (n+\tfrac{1}{2})\ln\xi(z) - \tfrac{1}{2}\ln K(z) + K_2 \tag{A16}$$

$$F(z) = D(z)\{K_3\xi(z) - \delta(z)\} \tag{A17}$$

where K_2 and K_3 are also integration constants.

If we consider an input beam with the field distribution function $U(x,0)$ as given by (7) in the text and determine the integration constants a_1, a_2, b_1, b_2, K_1, K_2, and K_3, we can uniquely determine the unknown parameters $A(z)$, $B(z), \cdots, F(z)$, and hence from (A1) the field distribution function $U(x,z)$. As a result, the primary parameters governing the propagation behavior of the light beam, the wavefront coefficient $1/S^2(z)$, the trajectory of the beam center $\delta(z)$, and its slope $\delta'(z)$ are obtained as (8), (9), and (10) in the text, respectively. From the definition of the wavefront coefficient, the spot size $w(z)$ and the curvature of the phase front $1/R(z)$ of a Gaussian beam are calculated as

$$w(z) = 1/[\mathrm{Re}\,\{1/S^2(z)\}]^{1/2}$$
$$1/R(z) = \mathrm{Im}\,\{1/S^2(z)\}/K(z). \tag{A18}$$

It is interesting to observe that the differential equations for $w(z)$ and $1/R(z)$ as well as the beam trajectory $\delta(z)$ conform with those derived from the viewpoint of ray theory. To derive the equations for $w(z)$ and $1/R(z)$, let the unknown parameter $A(z)$ be expressed as

$$A(z) = -\tfrac{1}{2}\{1/w^2(z) + jK(z)/R(z)\}. \tag{A19}$$

By substituting (A19) into (A6a) and equating the real and imaginary parts, respectively, we have

$$K(z)\left\{\frac{K'(z)}{R(z)} - \frac{K(z)R'(z)}{R^2(z)}\right\} = \frac{1}{w^4(z)} - \frac{K^2(z)}{R^2(z)} - g^2(z)K^2(z) \tag{A20}$$

$$\frac{1}{R(z)w^2(z)} = \frac{1}{w^3(z)}\frac{dw(z)}{dz}. \tag{A21}$$

From (A21) we get

$$\frac{1}{R(z)} = \frac{1}{w(z)}\frac{dw(z)}{dz}. \tag{A22}$$

Substituting (A22) into (A20), we obtain the equation for the spot size as

$$\frac{d^2w(z)}{dz^2} + \frac{G'(z)}{G(z)}\frac{dw(z)}{dz} + g^2(z)w(z) - \frac{1}{K^2(z)w^3(z)} = 0. \tag{A23}$$

Differentiating (A22) yields

$$\frac{d}{dz}\left\{-\frac{1}{R(z)}\right\} = \frac{-1}{w(z)}\frac{d^2w(z)}{dz^2} + \left\{\frac{w'(z)}{w(z)}\right\}^2. \tag{A24}$$

From (A23) we get

$$\frac{1}{w(z)}\frac{d^2w(z)}{dz^2} = -\frac{G'(z)}{G(z)}\left\{\frac{w'(z)}{w(z)}\right\} - g^2(z) + \frac{1}{K^2(z)w^4(z)}. \tag{A25}$$

Substituting (A25) into (A24) with (A22), we have the equation for the curvature of the phase front as

$$\frac{d}{dz}\left\{\frac{-1}{R(z)}\right\} = g^2(z) - \frac{1}{K^2(z)w^4(z)} + \left\{\frac{-1}{R(z)}\right\}^2 - \frac{G'(z)}{G(z)}\left\{-\frac{1}{R(z)}\right\}. \tag{A26}$$

The equation for the beam trajectory $\delta(z)$ is given by (A10).

We can easily verify that (A23), (A26), and (A10) agree with the results by the viewpoint of ray theory. For example, following Tien *et al.*'s paper [2], let us substitute the refractive index corresponding to the permittivity (1) in the text, $n(x,z) = n_0G(z)\{1 - (g^2(z)/2)x^2\}$ into the ray equation (3) of [2] and approximate

$$\frac{1}{n}\frac{\partial n}{\partial x} = \frac{-g^2(z)x}{1 - g^2(z)x^2/2} \doteqdot -g^2(z)x \tag{A27}$$

$$\frac{1}{n}\frac{\partial n}{\partial z} = \frac{G'(z)}{G(z)} - \frac{g(z)g'(z)x^2}{1 - g^2(z)x^2/2} \doteqdot \frac{G'(z)}{G(z)} \tag{A28}$$

with the assumption that

$$g^2(z)x^2/2 \ll 1$$

$$\left|\frac{g(z)g'(z)}{1 - g^2(z)x^2/2}\right| x^2 \ll \left|\frac{G'(z)}{G(z)}\right|. \tag{A29}$$

Then we obtain (A10), from which (A23) and (A26) are readily derived, according to [2].

ACKNOWLEDGMENT

The author wishes to thank Prof. N. Kumagai of Osaka University for his continuing interest and encouragement.

REFERENCES

[1] T. Uchida, M. Furukawa, I. Kitano, K. Koizumi, and H. Matsumura, "Optical characteristics of a light-focusing fiber guide and its applications," *IEEE J. Quantum Electron.*, vol. QE-6, pp. 606–612, Oct. 1970.
[2] P. K. Tien, J. P. Gordon, and J. R. Whinnery, "Focusing of a light beam of Gaussian field distribution in continuous and periodic lens-like media," *Proc. IEEE*, vol. 53, pp. 129–136, Feb. 1965.
[3] Y. Suematsu and T Kitano, "Analysis of a tapered lens-like beam guide," Nat. Conv. Record Inst. Elec. Commun. Eng. Japan., no. 535, 1967.
[4] K. Nishida, Y. Nannichi, T. Uchida, and I. Kitano, "An avalanche photodiode with a tapered light-focusing fiber guide," *Proc. IEEE* (Lett.), vol. 58, pp. 790–791, May 1970.
[5] S. Yamamoto and T. Makimoto, "Equivalence relations in a class of distributed optical systems—Lens-like media," *Appl. Opt.*, vol. 10, pp. 1160–1163, May 1970.
[6] ——, "On the ray transfer matrix of a tapered lenslike medium," *Proc. IEEE* (Lett.), vol. 59, pp. 1254–1255, Aug. 1971.
[7] H. Kogelnik, "On the propagation of Gaussian beams of light through lens-like media including those with a loss or gain variation," *Appl. Opt.*, vol. 4, pp. 1562–1569, Oct. 1965.
[8] S. Sawa and N. Kumagai, "A new method of analysis of the waveguide consisting of a lens-like medium," *Trans. Inst. Elec. Commun. Eng. Japan.*, vol. 52-B, pp. 624–631, Oct. 1969 (available in English in *Elec. Commun. J.*, pp. 109–116, Oct. 1969).
[9] S. Sawa, "Propagation of light beam through lens-like media with complex permittivity," *IEEE Trans. Microwave Theory Tech.*, vol. MTT-23, pp. 566–575, July 1975.
[10] P.M. Morse and H. Feshbach, *Methods of Theoretical Physics*. New York: McGraw-Hill, 1953, ch. 9.
[11] H. Kogelnik, "Imaging of optical modes—Resonators with internal lenses," *Bell Syst. Tech. J.*, vol. 44, pp. 455–494, Mar. 1965.
[12] D. Marcuse, "Physical limitations on ray oscillation suppressors," *Bell Syst. Tech. J.*, vol. 45, pp. 745–751, May/June 1966.